Overcoming Delays and Enhancing Subjective Comfort in Virtual Environments

Pierre Awaragi
Department of Biomedical Engineering
McGill University, Montreal
July 1999

A thesis submitted to the Faculty of Graduate Studies and Research in partial fulfillment of the requirements of the degree of Master of Engineering

ABSTRACT

Through the study of the effects of Virtual Reality (VR) on human subjects, scientists have determined that the main cause of discomfort while experiencing VR is the time lag between the head movements and its corresponding scene changes.

The main purpose of this thesis is to study and to propose solutions to reduce VR effects. The proposed solution is an alternative controller based on a Proportional Derivative (PD) model. Compared with a simple Proportional Controller, the PD Controller offers several enhancements: namely, a larger bandwidth and a faster and more stable reaction time. The proposed controller will also reduce the physical side effects commonly experienced by users of Virtual Reality.

RÉSUMÉ

La multitude de recherches sur les effets de la Réalité Virtuelle (VR) a confirmé au scientistes que la cause principale de malaise durant les expériences de VR est le long délai entre les mouvements de la tête et le résultant changement de scène.

Le but principal de cette thèse est d'examiner et introduire une solution pour réduire les effets de VR. La solution proposée consiste d'un nouveau contrôleur basé sur une stratégie de type « Proportional Derivative » ou Proportionnel Derivé. Les principaux avantages de ce contrôleur incluent une bande passante plus large et un temps de réaction plus rapide et plus stable. De plus, le nouveau contrôleur promet de réduire les malaises physiques que les usagers de la Réalité Virtuelle resentent.

ACKNOWLEDGEMENTS

I would first like to thank God for giving me the mind and will to finish this thesis. I would also like to thank my knowledgeable supervisor, Dr. H. L. Galiana (Mimi), for all her patience and support during the realization of this project. I hope that I have met your expectations. I also owe a great deal of gratitude to Ross Wagner, without whom I could not have completed this project. Special thanks goes to Eric Johnson for helping to build and construct the necessary hardware, and to Jimmy Palatsoukas for testing many pieces of the hardware before giving them to me and whose advice helped me in the analysis of the system.

This thesis would not have seen the light of day if it were not for the constant encouragement of my parents. I am forever in your debt. Your pride in my achievements is a reward all by itself. Thank you.

A final thanks goes to my girlfriend Germaine for her encouragement and constant nagging for me to finish this thesis.

TABLE OF CONTENTS

LIST OF TABLES

LIST OF FIGURES

Chapter 1 Introduction

In recent years, advances in computer technology have made access to Virtual Environments (VE) much easier than it once was. Standing in line for hours at the local amusement park for a mere five-minute VR experience is a thing of the past. Virtual environments have evolved to the point where they have myriad shapes and appearances, including Virtual Reality (VR) and Telepresence. These technologies allow people to immerse themselves in the world of Jurassic Park or be transported onto planet Mars.

These days, fast personal computers allow generation of 3D environments with extremely smooth transitions. However, despite the advances in computers and processors, VEs have some inherent problems that only recently have come under scrutiny. Many people who experience VR also experience fatigue, nausea, headaches, eyestrain, and, in extreme cases, vomiting and fainting.

Head tracking, according to a number of research projects, is the main cause of negative side effects while in a virtual environment. Latency and noise contamination are some of the other problems associated with conventional head tracking using magnetic fields2 [4] [6] [10][15].

Traditionally, VEs have been based on a Proportional Controller (PC) where the visual scene changes are linearly related to the movements of the user's head. In this thesis, the effects of head tracker latency on users of Telepresence will be presented. A new controller based on the Proportional Derivative (PD) controller will be proposed and tested in the context of a Telepresence environment. Results will show that the proposed controller can

and does reduce the degree of side effects experienced by users of VEs under the traditional Proportional controller. The PD can also be used in VR to determine how the 3D scene is to be generated.

To my knowledge, no such controller has ever been implemented or studied in the context of VE. Much of the research on virtual environments has been to determine the causes of side effects, to quantify them, and to determine the susceptibility of people to VR, but no effort has been made to try to eliminate or minimize such side effects.

It is the objective of this thesis to show that simply by implementing a smarter controlling scheme, the total system latency can be reduced and hence the side effects experienced by VE users can also be reduced.

Chapter 2 BACKGROUND

In this chapter, a brief background on Virtual Environments and the human visual system will be presented.

2.1 Human Visual Targeting System

The human visual system is a very complex system comprised of many subsystems, all interacting together to create accurate information about the surrounding environment. The main component of this system is the light sensors found in the back of the eyeball. The distribution of these light sensors (rods and cones), however, is not linear and is concentrated around a central area, the fovea. The fovea typically spans 2 spatial degrees, hence the accurate coverage of the surrounding scene is limited to that area. This is where the visual targeting system comes in.

The components of the visual targeting system are described next.

2.1.1 Vestibulo-Oculo Reflex

In its simplest form, the Vestibulo-Oculo Reflex (VOR) is responsible for stabilizing the visual scene on the retina during head movements. This is equivalent to maintaining a constant gaze direction. Gaze is defined as the orientation of the eyes relative to space. Gaze can also be described as the sum of the orientation of the eyes relative to the head and the orientation of the head, relative to space. Figure 1 is a graphical representation of the definition of gaze in space.

This reflex uses head motion, as sensed by the vestibular system, to cause oppositely directed eye movements. It is well described as a high-pass system of eye velocity relative to head velocity, with a break frequency near 0.1 Hz.

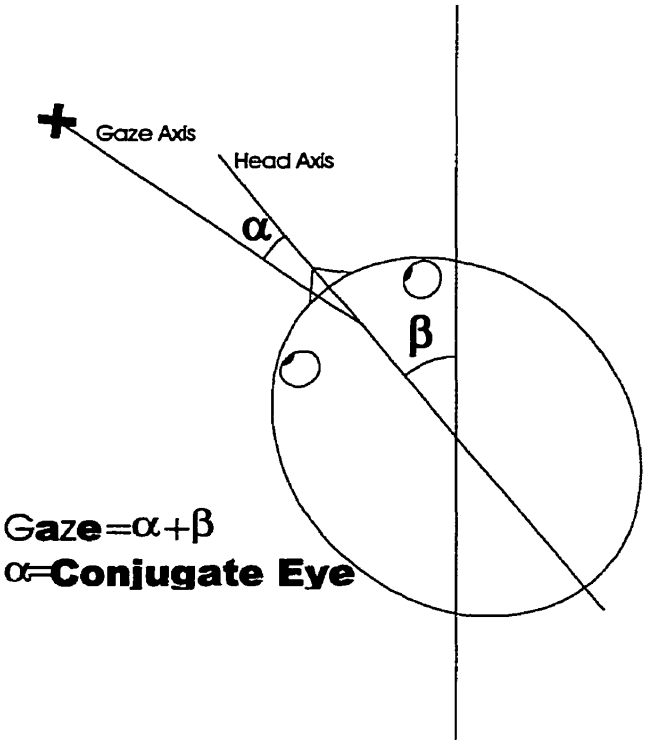

Figure 1: Gaze in Space

The VOR forms only a part of the visual targeting system. Optokinetic, saccades, smooth pursuit and vergence systems all interact dynamically with the VOR to bring visual targets onto the fovea and to stabilize them there [6][8].

2.1.2 Optokinetic Reflex

The Optokinetic Reflex (OKR) uses visual feedback to maintain a stable image on the retina. The entire retina, and not just the fovea, provides the visual feedback. Here, image slip (target velocity – eye velocity) acts as the main stimulus to the system.

Contrary to the VOR, the OKR acts as a low pass filter with a very low cut-off frequency between 0.1 and 1 Hz. The combination of OKR and VOR allows image stability from a very low frequency (due to OKR) to a high frequency (due to VOR).

2.1.3 Smooth Pursuit

Similar to the OKR, the smooth pursuit system uses visual feedback from the fovea (not the entire retina) to keep the image stable on the fovea. The movements of the eyes during smooth pursuit are based largely on the velocity of the visual target. Predictability of target motion will yield a better performance and a larger bandwidth.

Under normal circumstances, both VOR and smooth pursuit can occur simultaneously. According to research, when smooth pursuit goals counter those of the VOR, a phenomenon known as VOR suppression occurs. An example is during rapid reorientation of gaze orientation (saccades). This is valid up to approximately 1 Hz [1][6].

2.1.4 Saccades

Saccades are fast eye movements that allow rapid alignment of the target on the fovea using visual feedback. Once the visual target has been acquired and moved onto the fovea, smooth pursuit takes over to keep the target on the fovea.

Contrary to popular belief, saccades are not purely fast smooth pursuit movements, rather they are governed by a different logic, and rely on specialized brainstem circuits. (e.g. Gisbergen paper)

2.2 Virtual Environment

2.2.1 Desktop 3D Environment

In the old days of 3D movie theaters, two images representing the projections on a left and a right camera were **superimposed** on each other using the odd field lines for one image, and the even fields for the other image. These images were then split back at user level via special colored glasses.

Presently, a video projection system (typically a computer monitor) projects the two images representing the left and right cameras one after the other at twice the normal video rate (typically 60 Hz). A pair of Liquid Crystal Display (LCD) shutter glasses synchronized with the video projection alternately blocks either the left or the right eye. The overall effect is that each eye perceives only its associated image. The overall refresh rate is ½ of the projection rate (typically 30 Hz).

Such systems are used primarily for projection; no interaction with the user is allowed.

2.2.2 Augmented Environment

See-through head mounted displays are often used to allow viewing and interaction with real objects while simultaneously viewing virtual images. A good example of such a system is the Night Vision System (NVS) used in the Apache Helicopter, where the pilot is presented with a multitude of vital information.

No user interaction with the display is usually available in such an environment. Moreover, several problems arise in such systems regarding different focusing planes.

2.2.3 Virtual Reality

As the name implies, VR is a generated reality, a simulated environment in which we can voluntarily immerse ourselves.

Virtual reality presents the user with a computer-constructed scene. Any change in the orientation of the user will cause the regeneration of the scene. Such changes are normally

detected using head trackers mounted on the Head-Mounted Displays (HMD), which are also used for scene projection and display.

Since its inception, users of VR have complained of physical side effects, such as nausea and headaches. The main cause of discomfort in VR has been attributed to the time lag between the change in head orientation and the scene update on the HMD[10][15]. This lag can be due to the sum of several delays, including sensory latency, low sampling rate, video refresh rate and complex scenery computation time. Advances in technology have reduced the latter to the point where changes in scenery are quite smooth and not perceivable. New sensors that will reduce the latency and will increase the sampling rate of head movements are also being developed (see section 3.2.3).

2.2.4 Telepresence

A Telepresence system presents the user with images obtained via remotely mounted cameras. The change in head orientation yields a change in the orientation of the remote cameras. The main objective of Telepresence is to transport the user to other locations; such as the underwater world, inside a nuclear reactor, on the moon, or even on Mars.

The overall system experience is very similar to that of Virtual Reality. The inherent delays between head movements, camera movements and video refresh rate all contribute to the time lag responsible for most of the side effects.

Although similar in function, and though most of the conclusions drawn from one apply to the other, only Telepresence will be the subject of this thesis. Nonetheless, most of the analysis and conclusions can be applied in the context of VR.

2.3 Human Measurement Hardware

Available hardware in the laboratory would provide 3D tracking of eye and head movements, and 2D actuation of each of 2 remote cameras and a "head" (6D total). However, the main emphasis of this project was to explore feasible avenues to reduce the negative effects of delays in Telepresence. Hence, for the sake of simplicity without loosing the capacity to address the question at hand, the dimensions of the problem were reduced. In order to simplify the real-time controller, the measurement hardware and the remote system, the Telepresence system was implemented to interact only in yaw (1D). The measurement of the eyes' position was simplified down to only the composite version and the measurement of the head was restricted to yaw (rotation around the head's vertical axis).

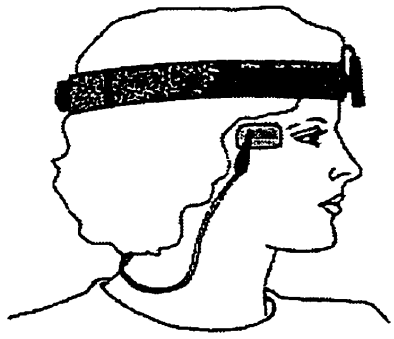

•Figure 2: Subject with Head and Eye Trackers

2.3.1 Eye Tracking

Several methods for measuring the position and velocity of the eyes currently exist. These include Electro-Oculography (EOG) and infrared video monitoring. EOG was chosen for this project.

EOG is the most frequently used technique for clinical and experimental evaluation of eye movements (position and velocity). This technique involves measuring the projection

of the polarized electric dipole of the eye globe along a pair of electrodes. As the eye moves, the orientation of the electric dipole changes and so does its projection. It has been shown that the changes detected by electrodes placed in the peri-orbital area on each side of the eye are proportional to the amount of displacement of the globe through a cosine function. When the electrodes are placed on opposite sides of the head to measure the pooled effect of both eyes (version or conjugate movements), the EOG voltage is linearly related to eye rotation up to approximately 50 degrees leftward or rightward from the midline. It can be recorded with little or no distortion by the use of DC amplifiers, with a resolution of ~2 degrees [22].

Another common measurement method involves monitoring eye position by infrared video cameras using diachronic mirrors inserted between the lens and the eyes. This method, although it allows for the free movement of the head, does change the head's inertial characteristics. Other very accurate techniques, such as coils embedded in contact lenses, were not considered since they required an immobilized head, and are invasive.

The EOG was chosen as a tracking system because of its simplicity and accuracy. The hardware used has little or no effect on the natural eye and head movements. The resulting measurements are quite linear especially if only version is measured (the average of the eye positions is equivalent to the orientation of an eye in the center of the head).

Figure 3 shows a sample of an EOG calibration curve (degrees vs. volts).

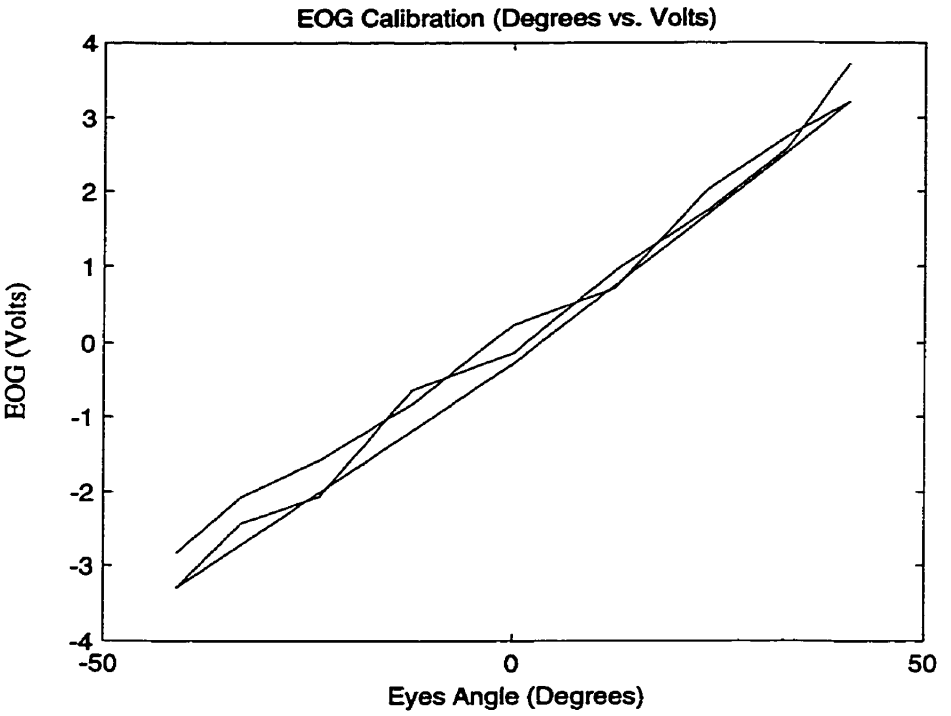

• Figure 3: Sample of an EOG calibration curve (Degrees vs. Volts)

2.3.2 Head Tracking

In order to localize the head in space, a head tracker measures either the position or the velocity of the head. Measurements are provided either in 1D, 2D or 3D. Different designs and methods are available. Common techniques include magnetic field sensors, Mercury liquid level detectors and inertial sensors.

An inexpensive commercial magnetic field sensor (using earth's magnetic field) was initially tested[1]. The data obtained was highly contaminated with noise and too sensitive to metal objects in the laboratory. Since only the head yaw was needed, a 1D inertial sensor was used instead.

---

[1] Part of the i-Glasses system made by Vio.

The head inertial sensor consists of two pairs of piezoelectric beam-bending elements, as shown in Figure 4. The sensor is attached to the head using a headband and outputs a signal proportional to the head's angular rotation rate. By integrating the angular velocity over time, the angular position is obtained. The main disadvantage of this kind of sensor is the constant drift, however small over time. This drift can be overcome by re-centering the entire system at fixed intervals. Another alternative for overcoming drift can be achieved by means of a magnetic compass also attached to the head[4].

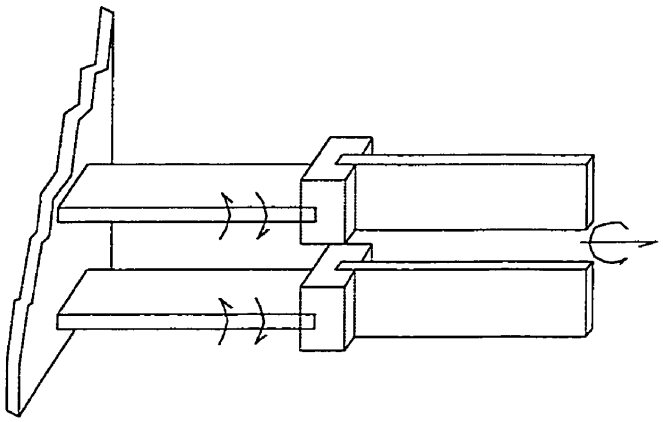

• Figure 4: Vorteq Head Sensor

Figure 5 is a sample of a recorded head and eye movement over time, which clearly demonstrates the higher noise levels in the EOG signals.

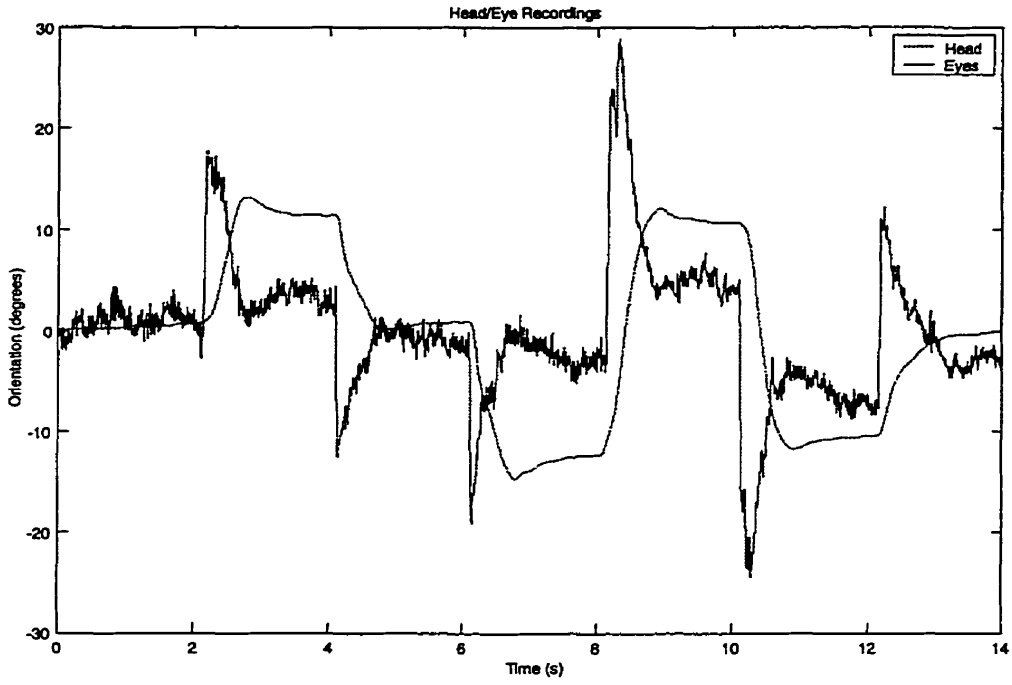

• Figure 5: Sample of Head and Eyes Recording Showing Clearly The High Noise Levels in The EOG Signals.

2.4 Head Mounted Displays

Head-mounted displays are a very convenient and practical way of presenting a 3D scene. HMDs are made of two small screens mounted on a headband along with a head tracker to provide computer software with the orientation of the head to be used in the creation of the visual scene. Generally speaking, HMDs have a relatively large field of view (typically 40 degrees horizontal and 20 degrees vertical). This field of view is obtained at the expense of image quality (typical screen resolutions are below VGA 640x480).

In Marran and Clifton[14], four designs are proposed to implement a good HMD that decreases the system's focus conflicts and increases the user's comfort level. (Pinhole optics, monocular lens addition combined with aniso-accommodation, chromatic bifocal and bifocal lens system, see [14] for a complete description of these systems). Only the adjustable and

fixed systems were considered for our HMD system. Table 1 summarizes the relevant characteristics of these two systems.

Fixed focal distance lenses with high diopter power (+10D to +40D) can allow the user to obtain clear vision without forcing a lot of accommodation. This system does not require any user training or precise adjustments. Problems arise with this system when small discrepancies (by fault of manufacturing) are introduced which the user cannot correct. These discrepancies include differences in diopter power of the two lenses, or inequality in the displacement between the two screens.

In the adjustable lens system, the user is given the task of adjusting for the manufacturing errors encountered in the fixed lens system which eliminate all related problems. This kind of adjustment, however, requires some training. The user can also introduce significant focusing errors (especially in low-resolution systems).

	Fixed Lens System	Adjustable Lens System
Lens' focal distance	Fixed	Adjustable
Sensitive to manufacturing faults	Yes	No
Requires precise focusing	No	Yes
User-dependant	No	Yes
Require training	No	Yes
Expensive	No	Yes

• Table 1: Comparison Between Fixed and Adjustable Lens Systems

The next chapter will discuss the current problems in Virtual Environments.

Chapter 3 Current Issues in Virtual Environments

As mentioned earlier, much research has been done and information is readily available with respect to the limitations and problems with current VR and Telepresence system designs. However, very little research has been done to correct and/or alleviate these problems and, of course, in order to improve upon a product, the product's problems and limitations must be thoroughly examined.

3.1 Current Problems/Limitations

3.1.1 Display Issues

Discrepancies in the design and mounting of fixed lenses in the HMD can change the focal depths of projected images causing the user to adjust accordingly, thereby forcing short- and long-term fatigue and discomfort. In the adjustable lens system where the user can adjust the distance between the screen and the lens, self-focusing features can also cause many symptoms of discomfort and fatigue both short- and long-term [14].

Screen resolution in HMDs tends to be poor. Most commercial units offer no more than a few thousand pixels per display (typically 300x200). This reduces Depth of Field (DOF) tremendously. An equivalent effect in Telepresence is apparent when remote cameras are not auto-focused but require manual adjustment thus limiting the DOF.

Other display problems might be the low video refresh rate resulting from the multiplexing of the two video images (to form a 3D signal). Typically, video refresh rates are in the 30 Hz range resulting in image flicker.

3.1.2 Accuracy and Susceptibility to Noise

Common commercial magnetic field head trackers tend to have lots of noise and are very susceptible to metallic objects or anything that has an electric field surrounding it (TVs, PC monitors, etc.).

Inertial sensors are used as head trackers by integrating angular velocity to obtain angular position. Integration over time results in drifts due to a signal DC bias. Precise inertial

sensors are also very sensitive to physical shocks and costs for repair are usually exorbitant, making them commercially unsound.

Using accelerometers as head trackers requires double integration (one for velocity and a second for position) which makes them very sensitive to DC bias, causing large drifts. Hence, the amount of drift on the signal of interest is much worse than that from inertial sensors.

3.1.3 Latency and Time Lag

As outlined in the section 2.2, VEs tend to have some inevitable delays built in. More often than not, one delay element is the head tracker. Inexpensive magnetic field head trackers have a large lag time, because of computational issues. Additional delay is introduced to the tracker signal when it is interfaced with the computer through an RS232 (serial port). Connection speeds are usually in the low 19600 Bauds producing a typical 75 Hz sampling rate.

Scene update time is also a factor in determining the total latency time in Telepresence. It is equivalent to the time required to send a camera's motor commands, for the motor to execute the commands, and for the video signal to return to the HMD. These delays can vary from a few milliseconds to as large as a few seconds for very remote systems (such as on Mars). In the case of VR, there is the time required for scene generation.

There is no question that the side effects experienced by users of VR are caused by the time lag between the head movements and visual scene updates on the HMD [6][15].

3.2 Current Work in VE

Constant work is being done to improve the overall experience of VE (especially in Virtual Reality). New technologies allow for constant improvement of individual system components. These include the following:

3.2.1 More comfortable HMD

New designs for HMD are providing a more ergonomic and comfortable setting for VE users. Lighter units mean that the user does not have to adapt to the additional weight. Higher resolution displays produce a better viewing experience, as well as a better DOF. One such new HMD is the DYHMD-B2000 by DAEYANG E&C which has an 800x600 points resolution at up to 75 Hz (www.personaldisplay.com).

3.2.2 Better System Designs

For a Telepresence system, having remote cameras with auto-focus capability does increase the DOF considerably. The addition of a distance estimator via laser or radar sensors provides the possibility for adding a more natural variable vergence setting. Lighter cameras, and faster, more responsive motors reduce any mechanical vibration resulting from fast moves.

For VR, faster processors produce smoother scene transitions with higher definition. Creating complex scenes (therefore or also) produce a more natural looking environment for the user.

3.2.3 Better Head trackers

E. Foxlin at the Sensory Communications Group is developing a new head tracker at MIT Research Laboratory of Electronics with funding from NASA [4]. This tracker offers

many advantages such as fast updates and the fact that it is self-contained giving it limitless range. The tracker is in essence an inertial tracker based on gyroscopes. The gyroscopes measure the angular changes directly with about one millisecond processing latency.

The tracker does, however, have its limitations. The small and inexpensive components that make up the tracker are not always accurate. Due to integration of velocity to obtain position, errors accumulate and the tracker drifts a couple of degrees every minute. To compensate, the tracker contains a compass and an inclinometer, which periodically take reference readings. Each time the user's head is still for a few moments, the tracker slowly resets itself to the orientation shown by the compass and the inclinometer.

A similar head tracker is used for the purpose of this thesis. It does not include a compass or an inclinometer but is reset by the user when necessary.

Chapter 4 Our Implementation of Virtual Environment

In order to implement the virtual environment, two cameras are used for the visual input. Their output is then combined using a 3D video multiplexer that feeds into the HMD video input mounted on the operator's head. A sensor is used to track the velocity of the user's head, and its output is converted to digital form using an Analog to Digital (A/D) card and then processed by the CPU. The results of the computations are converted to analog voltage via a Digital to Analog (D/A) card and are used to control the servomotors using the servo controllers. The servos dictate the orientation of the two cameras thus closing the loop. Figure 6 shows the different subsystems and how they are connected.

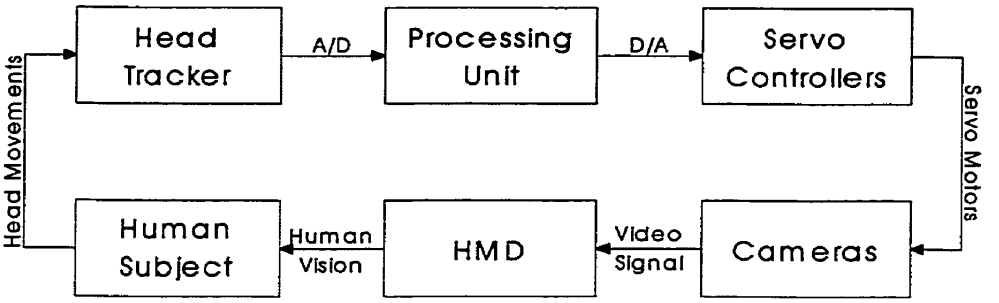

Figure 6: Virtual Environment System

A description of the individual subsystems follows.

4.1 Central Computing Unit

The central computing task is given to a Pentium 200 MHz MMX based personal computer with 128 Megabytes of Ram and 4.5 Gigabytes of hard disk. The operating software is Windows NT 4 with Service Pack 3. The hardware interface is achieved via National Instrument NIDAQ version 6.5 (This version of NIDAQ allows Windows NT 4 to interface two PC cards simultaneously). Code is written in Microsoft Visual Basic version 5.0 with National Instrument Component Works v1.1 ActiveX controls are used for interfacing with NIDAQ.

Another PC machine with a Pentium 133 MHz processor was used to provide visual targets for users. The visual images were projected using back-projection on a large screen made by 3M.

4.2 Head Mounted Displays

For the display of 3D scenes, a Virtual I/O (www.vio.com) unit was used. The unit has a pair of fixed lens displays, each with a resolution of 320x200 pixels. The typical field of view obviously depends on subjects and averages about 30 degrees in each eye.

The unit has two modes of operation: cinematic or VR. When in VR mode, an RGB signal (computer video output) serves as video input. A head tracker attached to the unit provides head orientation (3 degrees of freedom, pitch, yaw and roll). When in cinematic mode, the unit utilizes a 3D NTSC multiplexed signal to form the images on the left and right displays. The unit serves only as a 3D display in this mode. The head tracker is detached from the unit. Overall weight of the unit is approximately 250 g.

Further investigation of the quality of the unit's internal head tracker proved its data to be highly contaminated with noise. Furthermore the data transfer rate is not reliable or efficient since it depends on the serial port of the computer (RS232). For all these reasons, the HMD unit is used only in cinematic mode with a separate head tracker.

The HMD has the following manufacture specifications when in cinematic mode (video only):

- Heads-up see through distortion-free display
- Field of view: 30 degrees in each eye
- Fixed focus at 11' to minimize eyestrain
- Requires no IPD adjustment
- Can be worn with eyeglasses
- Two full color 0.7" LCDs
- Input: 1 NTSC channel, field sequential
- Resolution: 180,000 pixels per LCD panel
- Weight: 8 ounces
- Clip-on immersion visor
- Video: Single Channel RCA input

- True stereoscopic imaging
- Field sequential – flicker free

4.3 Head Tracker

An ARS-C141-1AR8P-600 unit based on the Watson angular velocity sensor and on the VORTEQ module (part of the VORTEQ VOR measurement system) was used as a head tracker. The tracker is based on an inertial sensor. The output of the unit is integrated to obtain a head angular position.

The output of the angular velocity tracker is an analog voltage with a linear range of ±10Vcorresponding to either ±200 or ±600 deg/s (switch-dependent). A DC component at the output must be subtracted to minimize the drift at the output of the integration (see Figure 7).

The angular velocity tracker is used only to measure the horizontal component of head movements (yaw). In order to measure the pitch and roll, two more would be needed.

The sensor has the following characteristics:

- Flat frequency response from DC up to 8 Hz.
- Sensitivity of ±600 deg or ±200 deg at full scale (±10 V).
- Linearity of 0.1% full scale.
- Averaged measured DC bias –25 mV.
- Radius of rotation independent.

- High Signal to Noise Ratio (SNR).

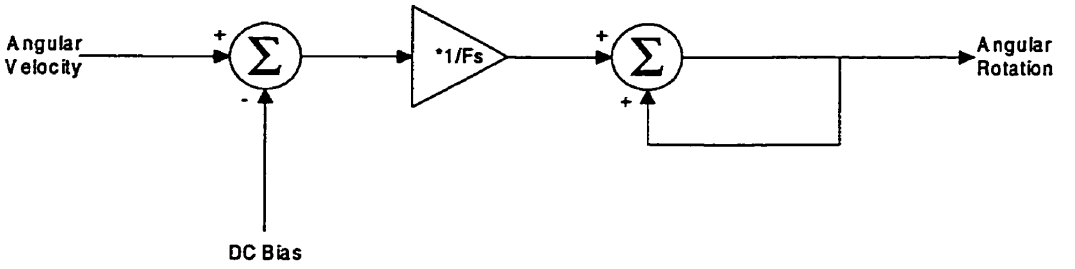

•Figure 7: Velocity Integration Logic to Estimate Head Position from Transducer's Output (Fs = Sampling Frequency)

4.4 EOG

One stage in the study required the measurement of both head and eye position of human subjects during natural gaze shifts to quantify operator's dynamic (refer to section 6.6). The angular position of the eyes was obtained using the EOG. Section 2.3.1 explains its principle of operation.

The EOG signal is obtained using disposable electrodes made by Physiometrix Inc (Hydrotrace Electrodes, MA). These electrodes have very good surface-skin contact thanks to a special gel. The electrodes feed into a first stage instrumental amplifier. The DC bias of the signal is eliminated on request (via a push-button or TLL binary voltage) using an integrator connected between the output of the instrumental amplifier and its reference input. The output of the first stage amplifier feeds into an optical buffer. The purpose of this optical buffer is to eliminate the feedback currents so as not to put the human subject in danger. Finally, the signal feeds into a final instrumental amplification stage with controllable gain and another DC bias eliminating integrator. The optical buffer chip supplies all the power needs of the amplifier stages in order to further reduce the risks of current leaking.

Before sampling the amplified EOG signals, anti-aliasing filters are used to attenuate the frequency content of the signal above 60 Hz. The 60 Hz cut-off frequency is chosen to reduce the 60 Hz electric humming present everywhere while preserving all the frequency content of the EOG (less than 30 Hz).

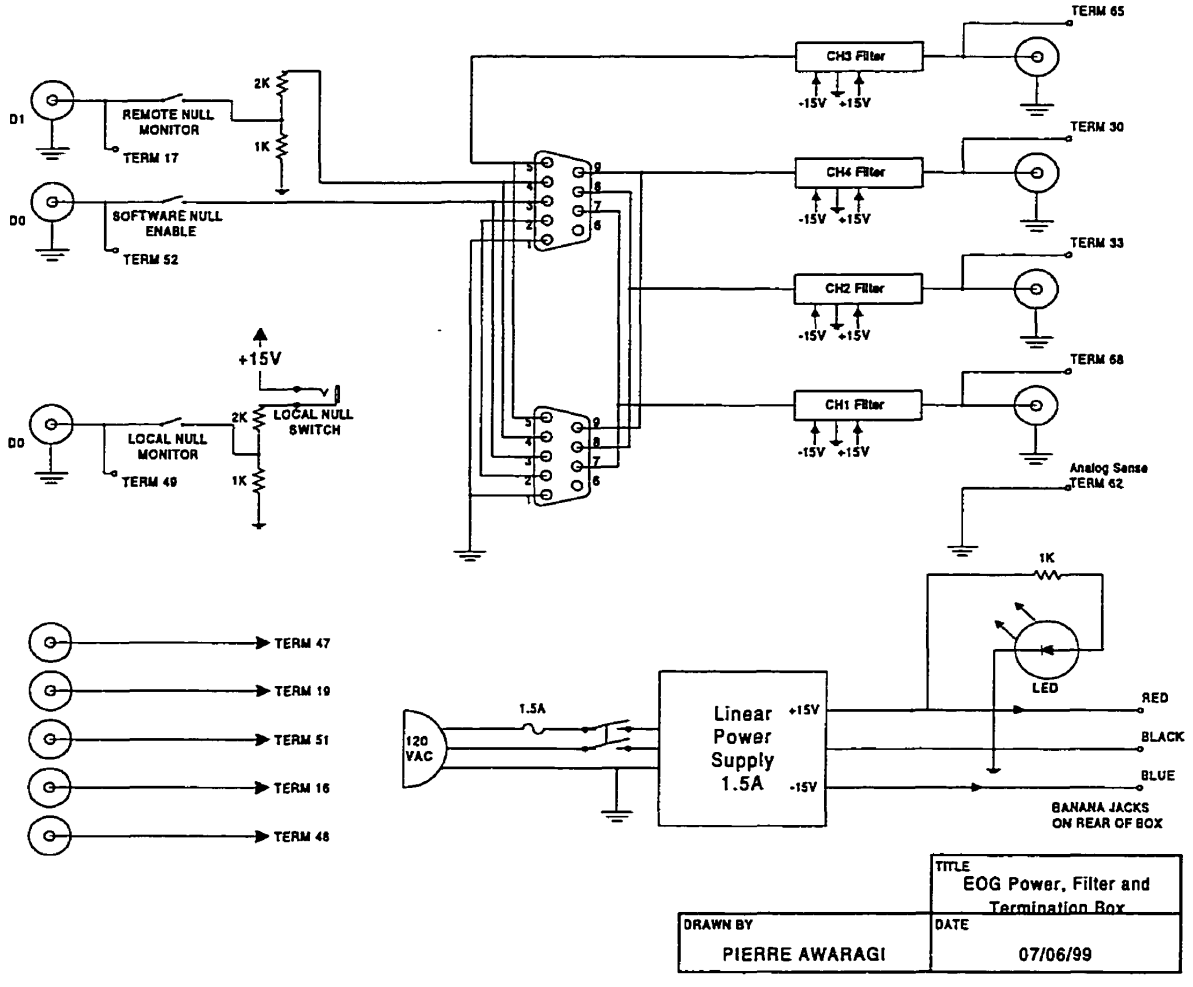

• Figure 8: Anti-aliasing Filters, Power Supply and Termination Box for Signal Conditioning Before Sampling of EOG Signals in Human Operator Study

The complete EOG conditioning system is designed to be modular. The preamplifier stage is contained (in pairs) in a single box that connects to a main power supply box also containing the anti-aliasing filters. Two preamplifier boxes can be connected to the anti-aliasing box to provide a complete eye tracking system (horizontal and vertical for each eye).

A reference signal is shared among all amplifiers. The main power supply box also provides a convenient one-connector plug to the A/D acquisition card along with monitoring BNC connectors (Figure 8).

The entire EOG hardware was designed and built in our laboratory. Next is the complete description of this system comprised of a preamplifier unit and a termination box containing anti-aliasing filters and power supply.

4.4.1 EOG Preamplifier

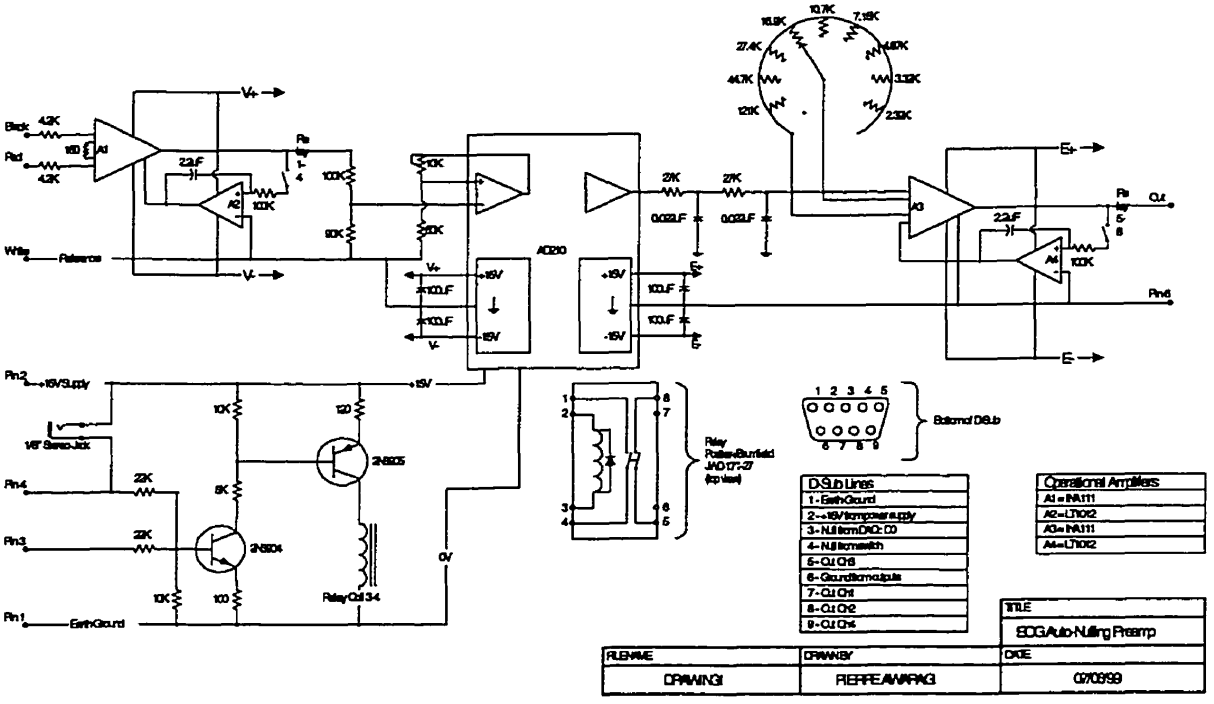

• Figure 9: EOG Preamplifier Circuit Diagram

The EOG preamplifier is provided with an auto-nulling feature because of the high propensity for drift in signals from surface electrodes. The auto-nulling feature is used in practice by having the subject stare at a reference point and pressing the hand-held switch for a few seconds. This will cause the capacitors across A2 and A4 to find voltages that will

generate a zero output voltage. When the subject's EOG baseline potential drifts, he or she can again stare at the reference and null the preamplifiers. Note that characteristic drift in the EOG potential is minimal after 20-30 minutes from first placing the electrodes.

The auto-nulling preamplifier consists of four sections: an input preamplifier incorporating the first part of the auto-nulling circuit, an isolation amplifier which also includes two ±15 volt isolated power supplies, an output amplifier which incorporates the second part of the auto-nulling circuitry, and a relay driver.

The relay driver is designed to pull in the relay coil when the input potential reaches TTL high level--about 2.5 volts. If a switch is inserted into the 1/8th inch stereo jack, the voltage at pin 4 (of the D-Sub connector) will rise to 15 volts. The 2N3904 transistor will saturate, turning on the 2N3905 transistor, and pulling in the relay.

In the part of the circuit involving A1 and A2, relay contacts 1-4 close when the relay is activated. The voltage on pin 5 of Al, which is an instrumentation amplifier, appears at the output of A1. (Recall that the equation of an instrumentation amplifier is $V_{out} = Gain \cdot (V^+ - V^-) + V_{ref}$.) The 100Ω resistor sets the gain at 500. A2 is an integrator. When relay contacts 1-4 are closed, any voltage on the output of A1 will cause a current to flow in the 100k resistor connected to pin 2 of A2. A2 is an almost perfect op-amp, so no current flows into pin 2. It can only flow into the capacitor. Pin 6, the output of A2, will have to move in the opposite polarity of the voltage on the output of A1. This voltage is added to the output voltage of A1 and brings the voltage at the output of A1 closer to zero volts. A2's voltage continues to change until no current flows into the capacitor. At this point, the output

voltage of A1 must be zero. In other words, any voltage generated at the output of A1 by an input voltage between pins 2 and 3 has been nulled. The subject can now release the button to open the relay contacts. Part one of the nulling has been accomplished.

A2 is almost perfect, but some current will flow into or out of pin 2 causing the capacitor voltage to drift. Notice that the output of A1 goes to a voltage divider, so that only 90% of its voltage goes into the input of the isolation amplifier. The input stage is configured as a non-inverting amplifier having a gain range of 1 to 1.2. Coupled with the attenuation of the voltage divider, the total gain is then adjustable from 0.9 to 1.08. Not only will the input voltage be adjustable over this gain range, but the drift rate of the capacitor will also be adjustable.

The AD210 isolation amplifier will transfer the voltage at the output of the input op-amp to the output op-amp at pin 1. The signal then goes through a passive 1 kHz filter into pin 2 of the second instrumentation amplifier, A3. Notice that the gain of A3 is adjustable in ten steps of 3 dB. Pin 2 is the inverting input. The reference (pin 5) is connected to zero volts. Pin 3, the non-inverting input, is connected to another integrator. The output voltage of A3, then, is $V_{Out} = Gain \cdot (V_3 - V_2)$.

The same concept is used to generate a nulled output voltage at A3: when the relay contacts close, the capacitor charges up to a voltage that produces a zero output from A3. The circuit is slightly different however. Instead of sending the nulling voltage to the reference, it goes into the non-inverting input of A3. As A2 and A4 drift, imagine both of them drifting together so that the difference will be zero.

Let the gain of A1 be G1.

The gain of the attenuator-non-inverter is G2.

The gain of A3 is G3.

The input offset is Vin-offset.

The drift of A2 is A2(t).

The offset at the output of the isolation amplifier is Viso-offset and the drift of A4 is A4(t).

The output voltage from A3 is Vout.

Thus, the equation of the output is:

$$\begin{aligned} V_{out} &= G_3\{[(G_1 \cdot V_{in-offset}) + (-G_1 \cdot V_{in-offset}) + A_2(t)] \cdot G_2 + V_{iso-offset} - V_{iso-offset} + A_4(t)\} \\ &= G_3[G_2 \cdot A_2(t) - A_4(t)] \end{aligned} \quad (1)$$

Now the reason for the adjustability of G2 is apparent. If A2 and A4 are selected so that they have very similar drift characteristics, the slight difference can be multiplied by G2 so that the last two terms of the equation cancel each other. The selection is not at all difficult because the op-amps are laser-trimmed and are all very similar to each other. The gain adjustment is also necessary because of tolerances in the values of the two capacitors.

4.5 D/A and A/D

Two National Instrument acquisition cards are used to perform all analog and digital I/O operations. The DAQCard-AI-16E-4 for the input, and the DAQ-1200 for the output.

The DAQCard-AI-16E-4 card has a total of 16 single-ended analog input lines, which can also be used as eight differential analog inputs (total of three input modes: differential, referenced, and non-referenced). All input gains are software-controllable and are

customizable per input channel. For the purposes of measuring the EOG and the head velocity signals, the card is configured as 16 single-ended, not referenced channels (NREF). For a complete list of available modes, see Table 2.

Along with its analog inputs, the card is also equipped with eight digital I/O ports that can be configured and used independently of each other. Digital output line 0 is used to activate the EOG preamplifier auto-nulling feature; digital input line 1 is used to monitor the hardware auto-nulling switch; and digital input line 2 is used to monitor a switch that can be used as a convenient set or reset button.

Input	Signal Source Type	
	Floating Signal Source	Grounded Signal Source
Differential (DIFF)	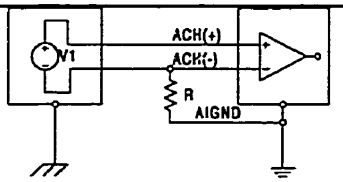 • Figure 10: Floating differential signal with bias resistor	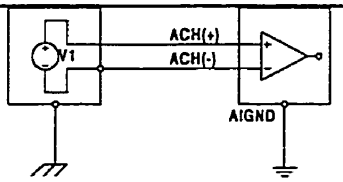 • Figure 11: Grounded differential input signal
Single-Ended-Ground-Reference (RSE)	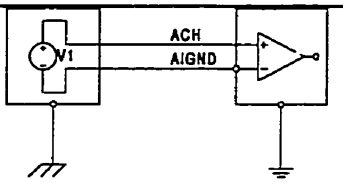 • Figure 12: Floating ground signal to ground referenced input	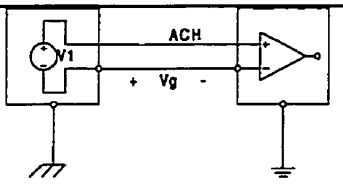 • Figure 13: Grounded signal to single ended ground referenced input (not recommended)
Single-Ended-Nonreferenced (NRSE)	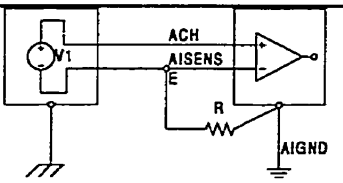 • Figure 14: Nonreferenced single ended input with bias resistor	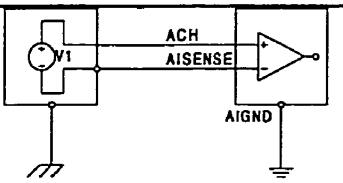 • Figure 15: Nonreferenced single ended input to grounded signal source

• Table 2: Input Modes for DAQCard-AI-16E-4 Card

The DAQ-1200 card has two analog outputs and eight analog inputs. The eight digital I/O lines form a single port that can either be set to input or output mode. All output and input channels have independent software-controlled gains. The card output line 0 is used to control the head servo command voltage. The output line is configured to be in the bipolar mode with a range gain of 1 for an effective voltage range of ±5 V.

Both cards are used in single point mode (send a request and wait for response). The two cards sustain a total of 300Hz sampling rate real-time.

4.6 Robot Head

The robot head serves as the remote version of the human user. Its main purpose is to orient the two cameras in the desired direction. The robot head is comprised of the servo motors used to move the cameras and the servo controller used to convert analog voltages from the D/A card to pulse commands for the motors.

4.6.1 Servo Motors

The design of the "Robot Head" allows for six degrees of freedom: Two for the "Head" and two for each of the "Eyes". Figure 16 shows the schematic for the Robot Head and its 6 degrees of freedom.

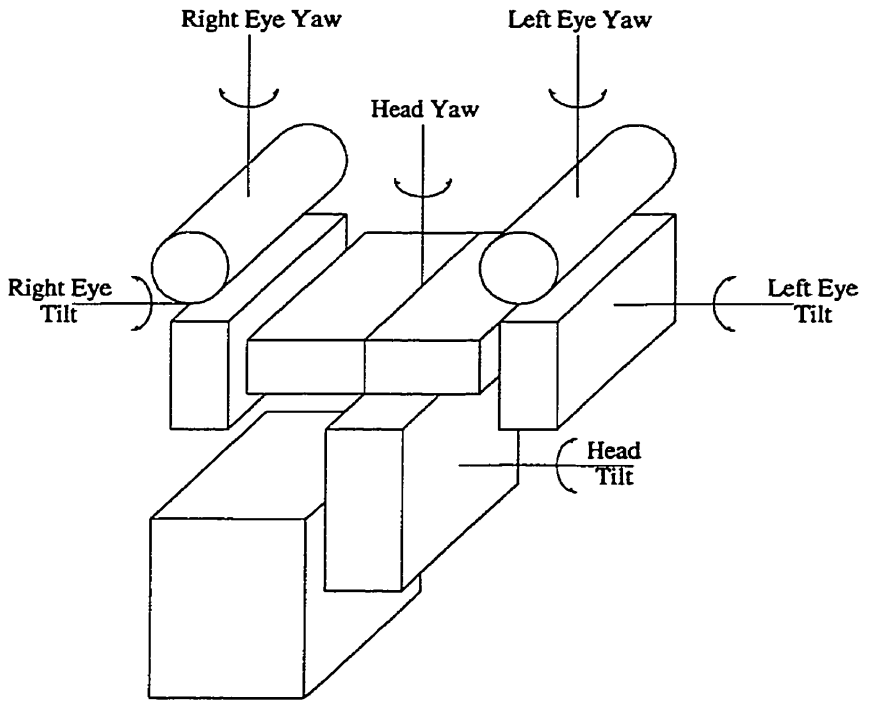

• Figure 16: Robot Head and its 6 Degrees of Freedom

The original design of the robot head was to use all six degrees of freedom but due to the limitation of the D/A card, a maximum of two motors can be controlled simultaneously via the computing host. For the purposes of a simple Telepresence system, only the head motor needs to be controlled via software. This is done only in the horizontal plane, thus a 1D design is obtained for yaw update.

For the 1D Telepresence system, the robot head is composed only of the head yaw servomotor. The two eye servomotors are used to adjust the version-set-point for each user and thereafter remain fixed.

Plant	Servo Model	Characteristics
Eye	Futaba S3101	Torque: 2.2Kg/cm Speed: 0.22 s/60° Size (W/H/L): 13/27/28 mm Weight: 17g Range: 180°
Head	NES-4721	Torque: 2.2Kg/cm Speed: 0.22 s/60° Size (W/H/L): 33/19/39 mm Weight: 49g Range: 180°

Table 3: Head and Eye Servo Motors' Characteristics

4.6.2 Servo Controller

The servomotors controlling cameras and robot head are active devices, meaning that they require constant driving or they return to their neutral setting (center position). They are controlled via a variable pulse width signal. A servo controller is used to convert analog signals to valid pulse signals. The full description of the servo controller can be found in [19]. In short, they provide 256 levels of orientation over a span near 180 degrees.

The servo controller is synchronized using a standard NTSC video signal from one of the cameras. The corresponding refresh rate is thus set to 60Hz. The input signal is calibrated to that of the bipolar output of the DAQ-1200 card: therefore,–5V corresponds to one extreme while the +5V corresponds to the other and the center position is obtained by a 0V.

4.7 Cameras

Two Elmo miniature camera systems form the eyes of the Telepresence system. The two cameras are mounted on the servomotors and their orientation is controlled via the servo controllers.

The Elmo camera system consists of a controller unit MN401E along with a C-Mount CCD camera head to which a C-mount lens can be attached. The characteristics of this system are listed below:

- 400,000 pixels CCD
- 9 Shutter speeds 1/60-1/10000
- Full Automatic White Balance control and manual setting

- Separate camera
- Internal/External Synchronization
- 60Hz NTSC output signal
- Camera head weighs 16g without a lens and 75g with a lens (without the extension cable)

Characteristics	F=3mm	F=7.5mm
Aperture	1:1.8	1:1.6
Field of View	88.6°×115.8°	38.4°×48.2°
Focusing Distance	10mm~∞	20mm~∞

•Table 4: Effects of Lens Focal Distance on Camera Properties

In order to provide a field of view through the HMD close to normal by matching the field of views of the HMD and lens, the 7.5mm focal distance lens was chosen (the visual scene actually appears slightly further away than it is supposed to, but remains within acceptable limits).

4.8 3D Video Multiplexer

In order to provide the HMD with its required 3D NTSC field sequential signal, the video signals produced by the two cameras must be synchronized and combined together. The synchronization part is completed by feeding the output of one camera into the external synchronization of the other camera creating genlocked cameras (a master-slave configuration).

A VREX Inc. stereo Multiplexer VR-MUX1 is used to combine the genlocked video signals into a one field sequential signal that feeds into the HMD. The output signal for each eye is thus refreshed at half the refresh rate of the original NTSC signal (30Hz).

Following the description of the hardware used in this project, the software for closed loop Telepresence will be presented in the following chapter.

Chapter 5 Proposed Controller

Traditionally, the orientation of a 3D camera system whether in VR or in Telepresence is dictated directly by the orientation of the head. Despite delays between the acquired movements of the head and the scene change, no compensation is used.

Research on the VOR has shown that any delays greater than 100ms between the movement of the head and changes in scene are perceivable. As described in section 3.1.3, one of the major components reducing comfort in Virtual Environments is the system lag or delay.

In this thesis, an alternative controller based on the Proportional Derivative controller will be proposed and used in an attempt to reduce any time lag present in the VE system, to increase the overall level of comfort.

First, a mathematical model of the VE system will be presented to allow simulation tests of potential controllers. Then a traditional proportional controller will be described along with its known limitations and problems. Finally, an alternative controller based on the Proportional Derivative scheme will be proposed and described. The focus here is to minimize the effects of delays. No compensation for hardware or human dynamics will be provided.

The following conventions will be used through out the rest of this thesis:

- h(t) represents human head orientation around its axis in space with respect to a fixed reference (degrees).

- v(t) represents head velocity as measured by the Head Tracker and sampled by A/D (Volts).

- x(t) represents the estimated head position after integrating of v(t) (Volts).

- y(t) represents the servomotor position command as computed by the system controller (Volts).

- p(t) represents the actual servomotor position around its axis in space with respect to the same head reference orientation (degrees).

5.1 VE System Modeling

This section describes the methods used to generate full simulation of the Telepresence system. The intent is to test the effects of several controllers in the context of a simulation of the Telepresence system. Using a model of gaze control to simulate the human operator, including Vestibulo-Ocular Reflex, a complete Telepresence system model can be synthesized and simulated.

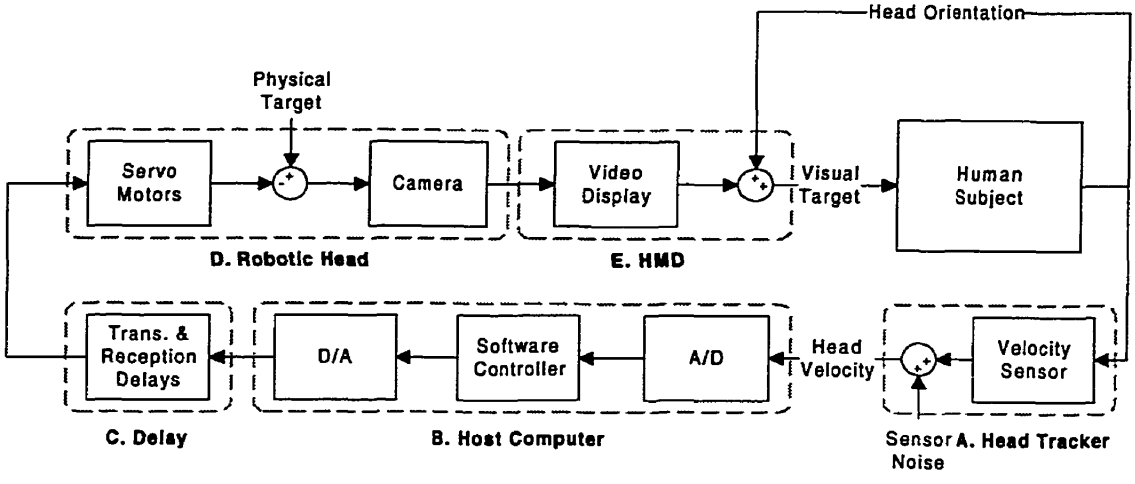

Figure 17: Telepresence System

A. Velocity sensor head tracker. B. Host computer with the controller. C. Transportation Delay. D. Servo controller, servomotors and cameras (Robotic head with Eyes). E. Head Mounted Displays

Figure 17 shows a schematic of a Telepresence system. This system is comprised of several subsystems. The hardware subsystems are all described in Chapter 4. Here the focus is on software controller and the human operator model. More detailed information on dynamic models of the hardware components are presented in Chapter 6.

The sampling rate of the system is set at 250 Hz. The normal Bandwidth (BW) of the human head is usually in the 5 Hz range, and the normal BW of human eyes is ordinarily

under 30 Hz. Hence, the selected 250 Hz sampling rate insures that head and eye bandwidths are fully covered.

One important point about this system is the feedback loop from the human subject to the HMD unit. Since the HMD is physically attached to the human head with the target located on the HMD (video image), any rotation of the human head will result in an equivalent movement of that target in the same direction. This is illustrated in Figure 18. This effect is opposite to that of the cameras mounted on the robotic head; hence, it is subtracted in the Telepresence schematic.

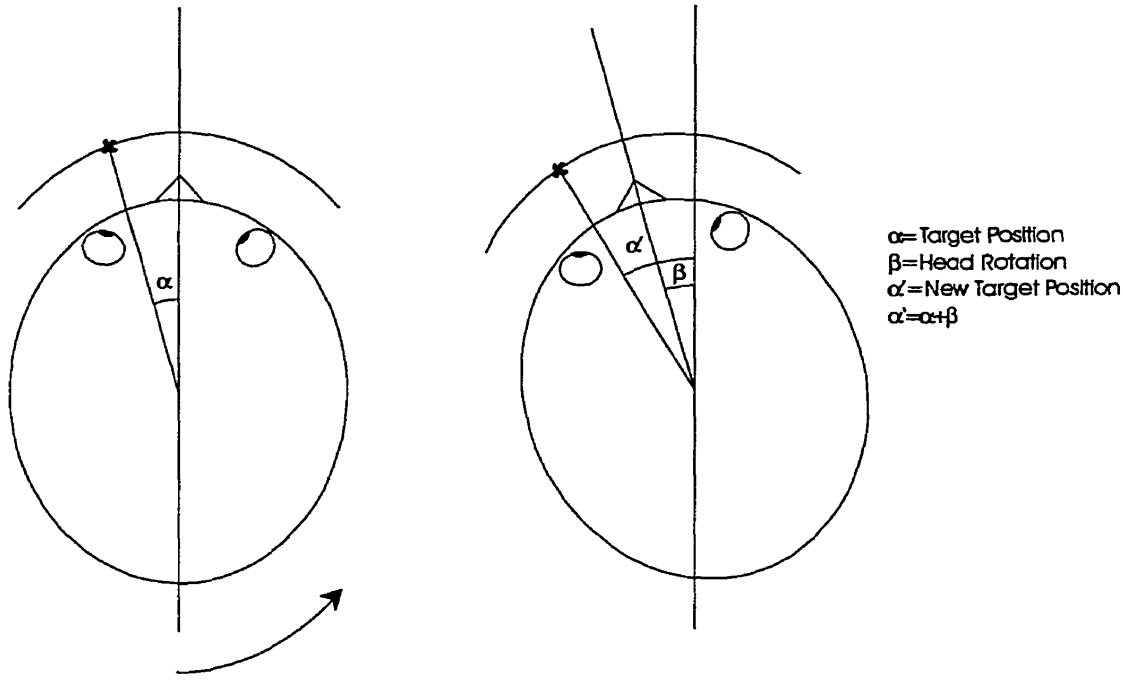

Figure 18: Effect of Head Movement on HMD's Target Spatial Location

Note that other VR systems can be just as easily described and modeled by applying the following changes to the Telepresence Model:

- Robotic head becomes computer-generated scene function of Software Controller output
- No need for the D/A phase
- Transmission and reception delays become scene generation delay, a function of scene complexity and computer performance.
- The host unit includes everything up to the HMD unit

5.2 Gaze Controller

Many gaze control schemes have been proposed to model human eye-head coordination, and the role of the VOR. A non-linear gaze controller developed by Dr. H.L. Galiana at McGill University will be used to implement a simulated human (refer to [8] for a full description of this model). The main purpose of this controller is to align the head and the eyes along a visual target over time in a manner similar to humans. The gaze controller assumes a single conjugate eye located at the same location as the head axis.

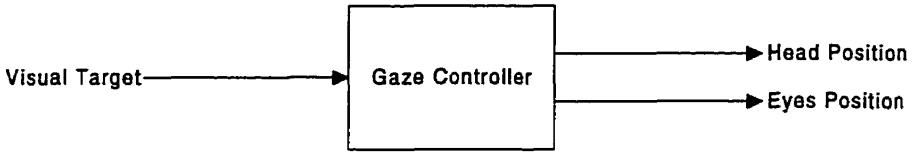

• Figure 19: Gaze Controller

This modeling approach has previously been used to control a binocular robot on a mobile head [19]. The model is reproduced in Figure 20, where the dashed lines represent activation of circuits elements only during saccades and the reminder of the circuit coordinate eye and head interactions during target fixation or slow pursuit.

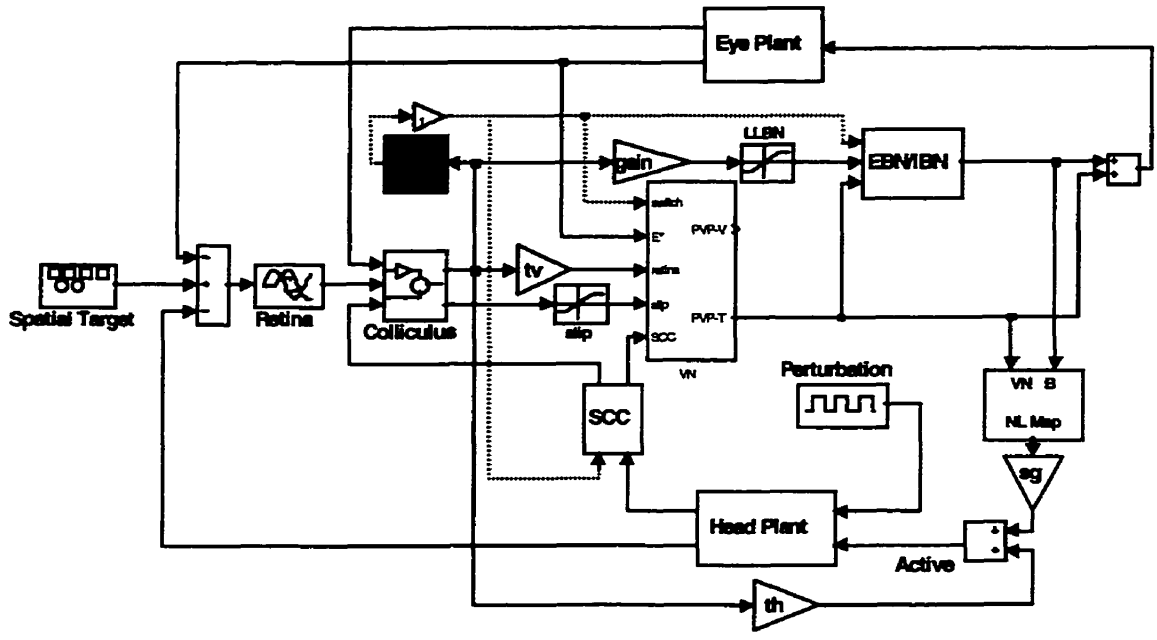

• Figure 20: Simulink Model of Human Gaze Controller. Shaded box is a Switch Controlling the Release of Saccades.

A typical head and eye response is illustrated in Figure 21 where the gaze controller is presented with a relatively large target. The parameter set used in the simulation here consists of the following:

- th = 1.0
- tv = 2.0
- sg = 3.0
- gain = 4.0
- SAT = 20.0

The trajectories could be tuned with different parameters to provide any desired final contributions (steady state) of eyes and head to the gaze shift, and appropriate saccadic dynamics, in order to match the behavior of any human without changing the model structure. Eventually this could be used to model the human operator in more advanced

Telepresence systems. Here it is used only to compare the performance of potential software controller in reducing the effects of delays.

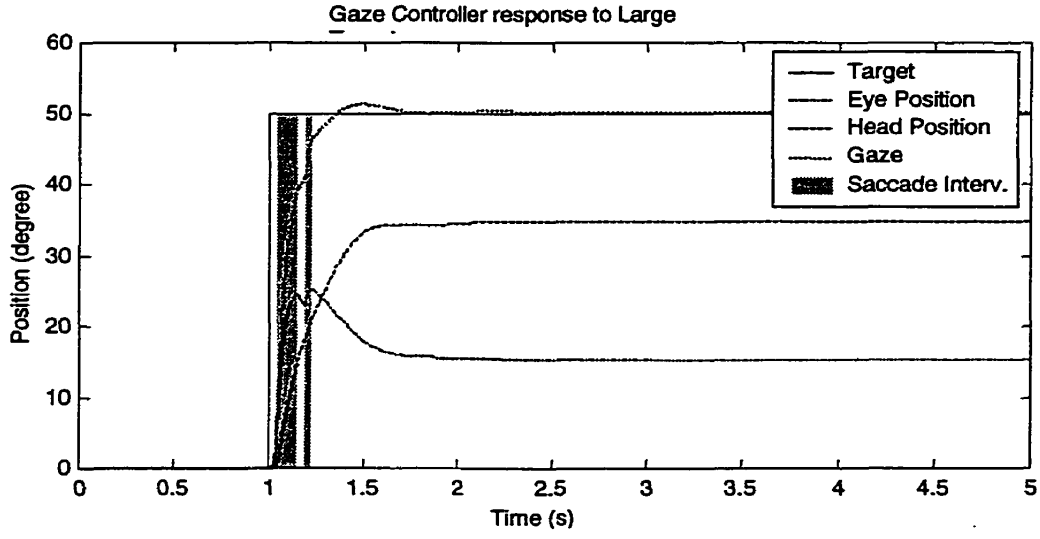

• Figure 21: Gaze Controller's Normal Response to a Large Visual Target (50 degrees)

5.3 Head Tracker Transducer Compensation

5.3.1 Description

Since the head tracker is a velocity sensor, its output voltage is expressed in terms of the head rotation as follows:

$$v(t)=\frac{dh(t)}{dt}$$
$$v[i]=\frac{(h[i]-h[i-1])}{\frac{1}{f_s}} \qquad (2)$$

where v is the sampled angular head velocity, and h is the head position. When expressed in z-domain the preceding equation becomes:

$$V[z]=f_s\left(H[z]-H[z]z^{-1}\right) \qquad (3)$$

Which results in a transfer function that is:

$$\begin{aligned} T_{HeadTracker}[z] &= \frac{V[z]}{H[z]} \\ &= f_s\left(1 \quad z^{-1}\right) \\ T_{HeadTracker}[z] &= f_s \frac{z \quad 1}{z} \end{aligned} \tag{4}$$

The analytical function representing the velocity integrator used to compensate for the head tracker transducer is expressed as follows:

$$\begin{aligned} x(t) &= \int_0^t v(l)dl \\ x[i] &= x[i-1] + \tfrac{1}{f_s} v[i] \end{aligned} \tag{5}$$

Where x is sensor voltage and y is estimated head position in sensor units. When expressed in the sampled domain this equation becomes:

$$X[z] = X[z]z^{-1} + \tfrac{1}{f_s} V[z] \tag{6}$$

This can be expressed graphically by the following figure.

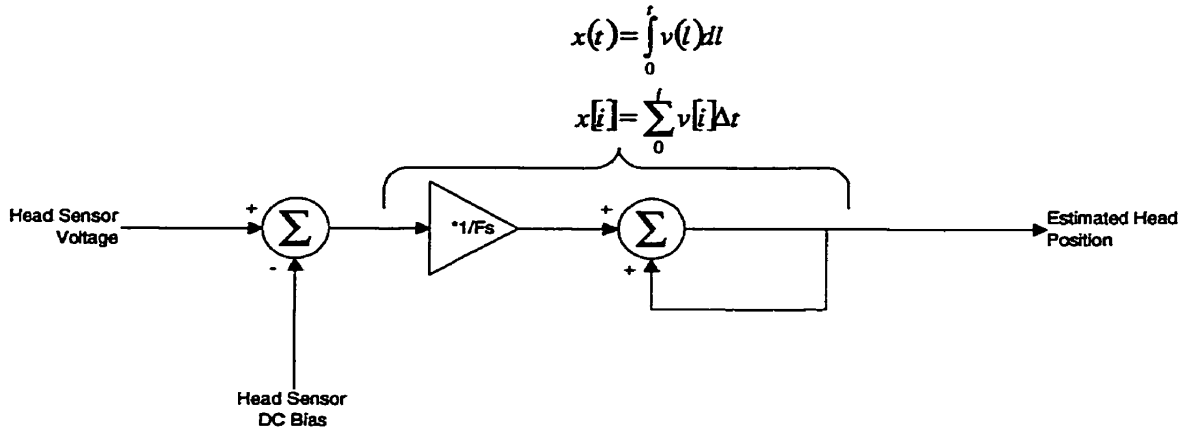

•Figure 22: Integration of Head Tracker Velocity to obtain Position

The system transfer function is expressed as the output function over the input:

$$T_{Integrator}[z]=\frac{X[z]}{V[z]}$$
$$=\frac{\frac{1}{f_s}}{1\quad z^{1}} \qquad (7)$$
$$T_{Integrator}[z]=\frac{1}{f_s}\frac{z}{z\quad 1}$$

Figure 23 shows the step response of such a transfer function while Figure 24 shows its frequency response (based on discrete system simulation).

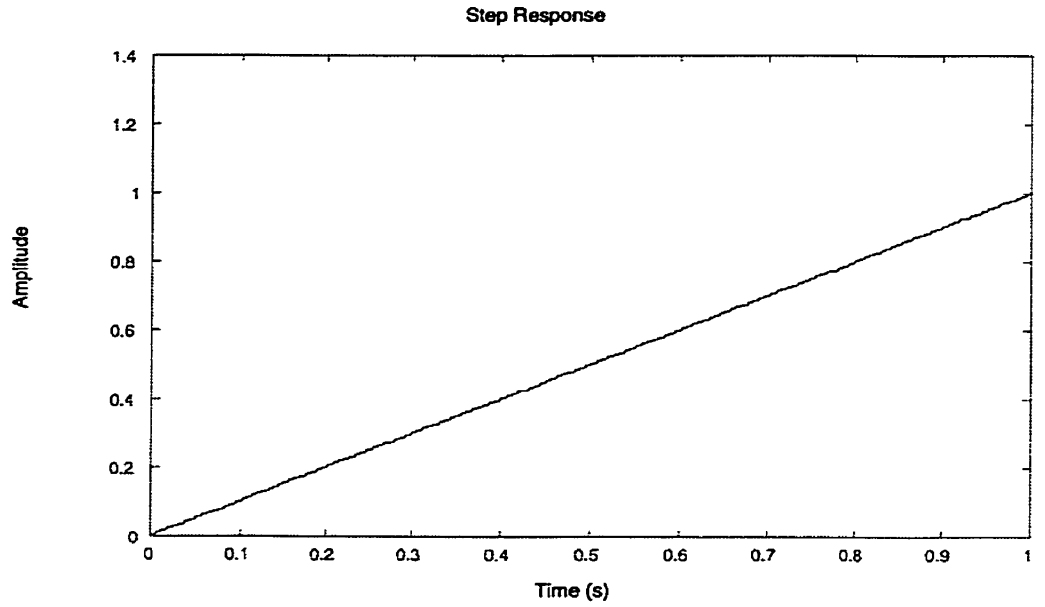

•Figure 23: Integrator Step Response

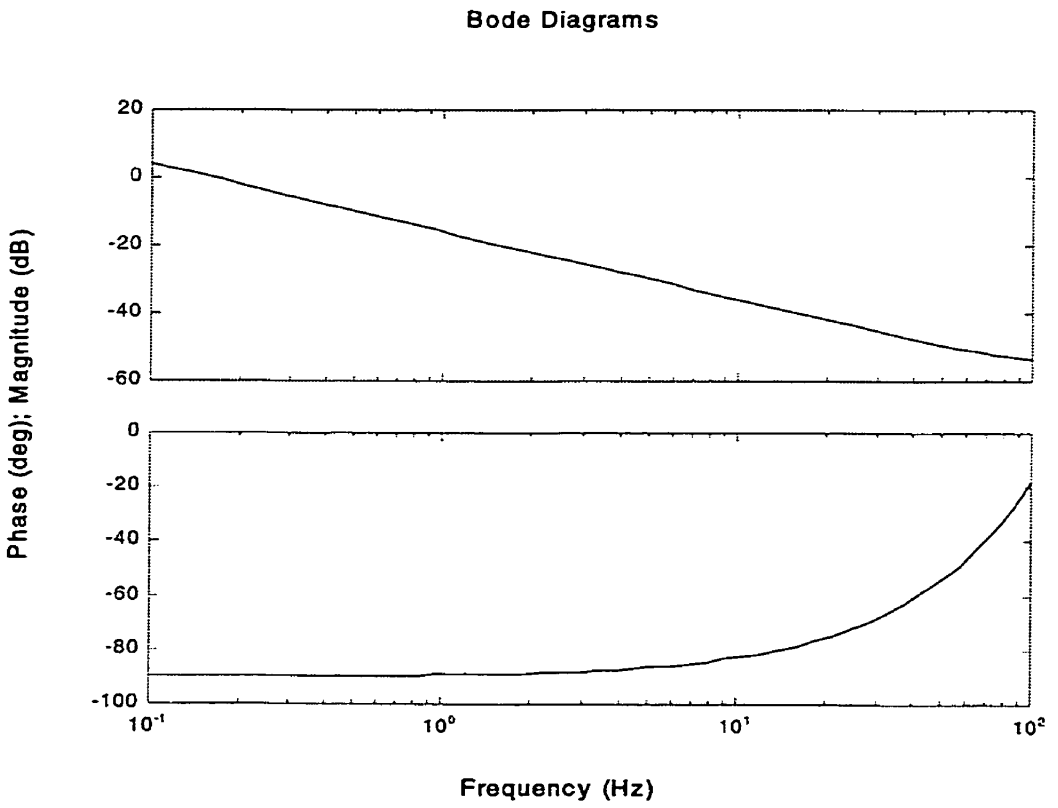

•Figure 24: Frequency response of the Implemented Integrator

Assuming perfect servomotors -ones that respond instantly to any position command when the head tracker transfer function combines with the Proportional Controller transfer function- all poles and zeros cancel out yielding an all-pass zero phase transfer function. The resulting system transfer function causes any rotations of the subject's head to result in a resembling rotation of the servomotors equal to it in amplitude and phase.

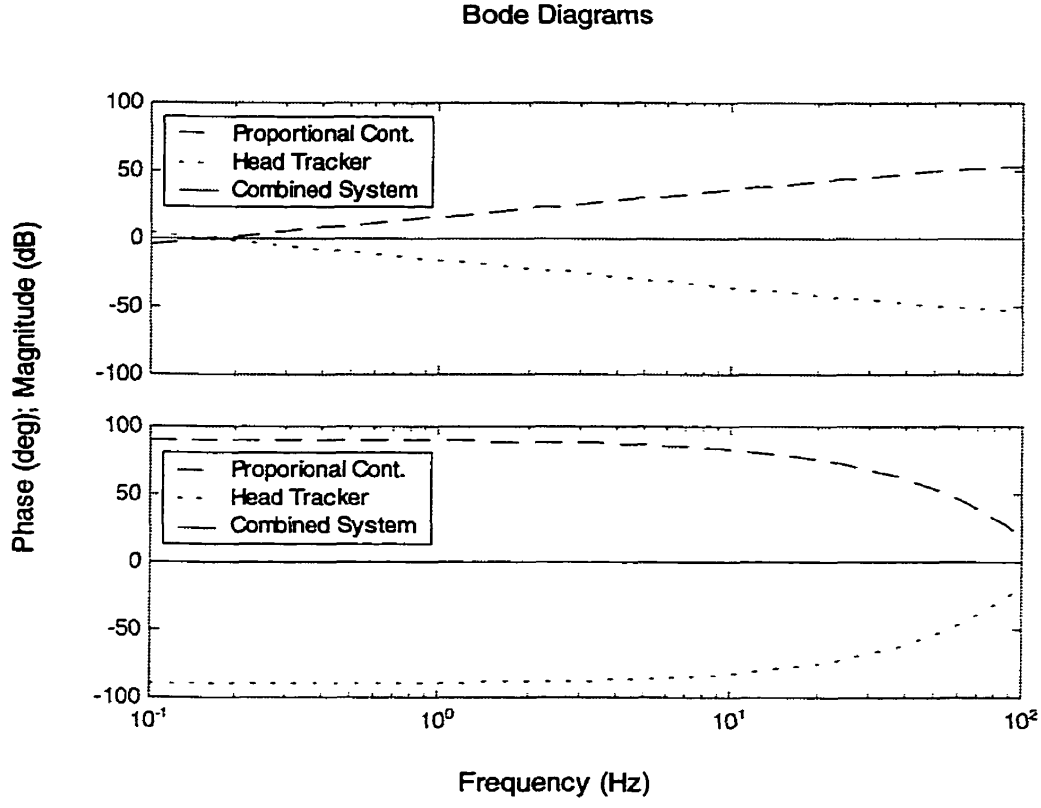

Figure 25: Frequency Response of Combined Head Tracker and Proportional Controller

5.3.2 Implementation

The software code flowchart of the controller is shown in Figure 26. A special capability to reset the bias in the digital integrator was embedded using one of the digital ports of the A/D.

The source code required to implement this compensator and user interface is provided in Appendix A.

Note the implementation of a manual reset capability using a mechanical switch monitored by a digital port on the A/D card. The importance of such capability arises from the constant drift caused by the integration of the DC bias of the head tracker.

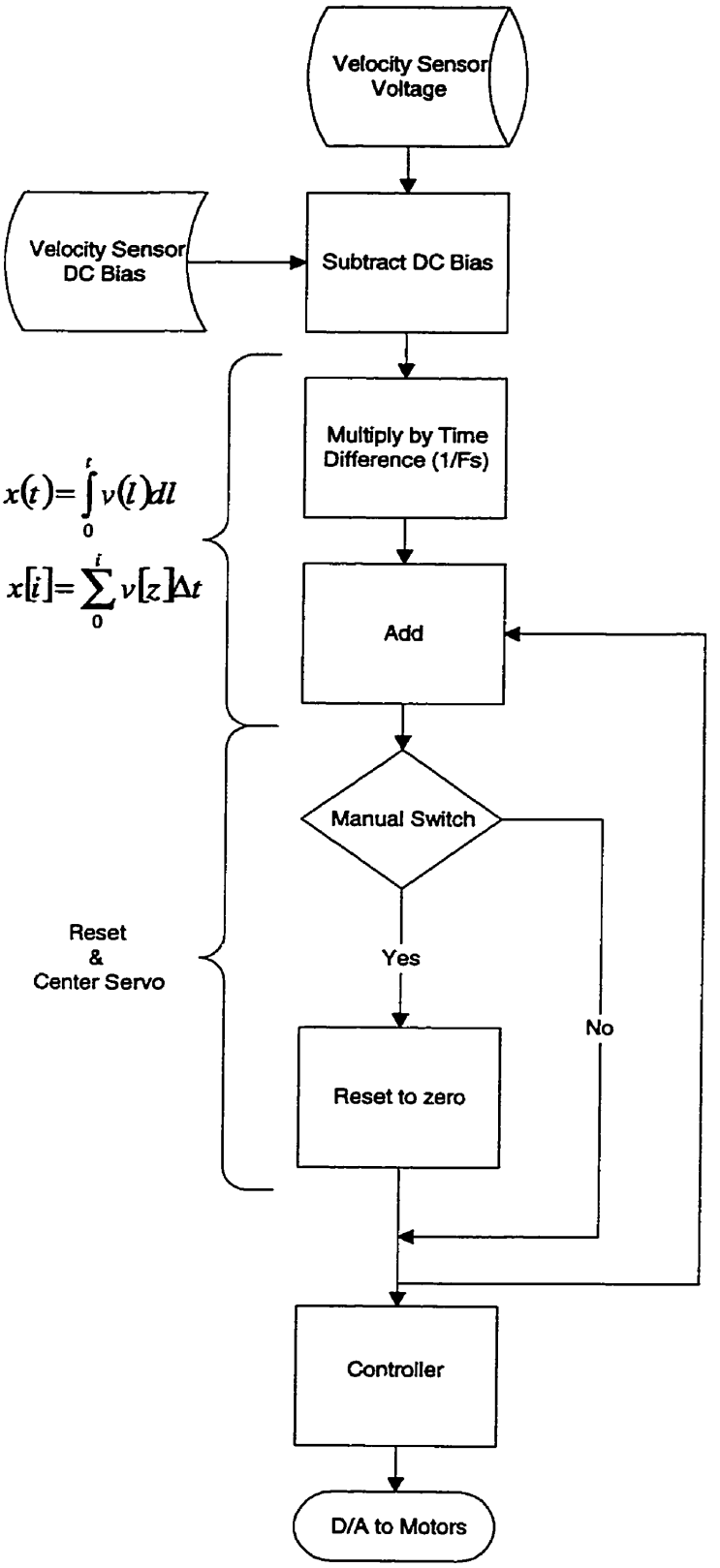

• Figure 26: Proportional Controller Code Flowchart

5.4 Proportional Controller

5.4.1 Description

The main purpose of a controller is to drive the output of its target system to a desired state based on controller input. The input in this simplest case is the estimated head position extracted from the velocity sensor. The output of the controller is a command voltage that drives the servomotors to a desired **position** through the D/A card running at the same sampling rate as the A/D card (250Hz).

As described in section 4.6, the voltage input of the servo controller is translated to rotation degrees following a linear relation: [-5V, 5V]→[-45°, 45°]. The voltage output of the velocity sensor is also related to head movement by a linear relation: [-10V, 10V]→[-600°/s, 600°/s].

Assume an idealistic world where no delays or non-linearities exist. Simply scaling the input to match its range with that of the output should produce the controller's desired effect: rotating the human head by a certain amount results in the movements of the robotic head by that same amount. Here no compensation for servomotor dynamics is provided since their BW is even larger than that of human head movements.

5.4.2 Known Limitations

If simplicity in coding is a main factor in the selection of a controller, the Proportional Controller represents the perfect choice. However, this type of controller has the following disadvantages:

1) No protection against sensor noises. This can be overcome at the expense of adding an analog filter just before the data acquisition board, but this can reduce the overall BW of the velocity sensor, meaning that certain quick head moves will not be observed.

2) An inaccurate DC bias can cause the current estimated head position to drift at a constant rate and depending on the error size, this drift can be quite large taking into consideration the high sampling rate. The DC bias of the velocity sensor can also change over time due to a number of factors, such as ambient temperature and insufficient averaging time. This sensor-related problem has no real solution but several workarounds. A longer averaging time can provide a more accurate reading of the bias. A manual reset button can allow the user to reset the system to center position, but this reduces the automation of the system. As mentioned in section 3.2.3, adding a magnetic compass to realign the system can bring the need for user intervention to a minimum.

3) Ideally, the frequency response of the entire head to robot system should be that of an all-pass with zero degrees phase lag. However, the velocity sensor and the servomotors are not perfect systems with built-in delays and noise contamination. Any transmission delays between the head tracker and the proportional controller will be added to those between the proportional controller and the servomotors. The resulting system will then have an all-pass behavior with phase lag. This can be expressed mathematically using a first order Padé approximation of a delay

element $T(s)=\frac{(-\tau/2)s+1}{(\tau/2)s+1}$. For a 100 ms-transmission delay. The transfer function of the Padé function is shown in Figure 27. As expected, the function has a constant amplitude response and a phase lag that increases with frequency.

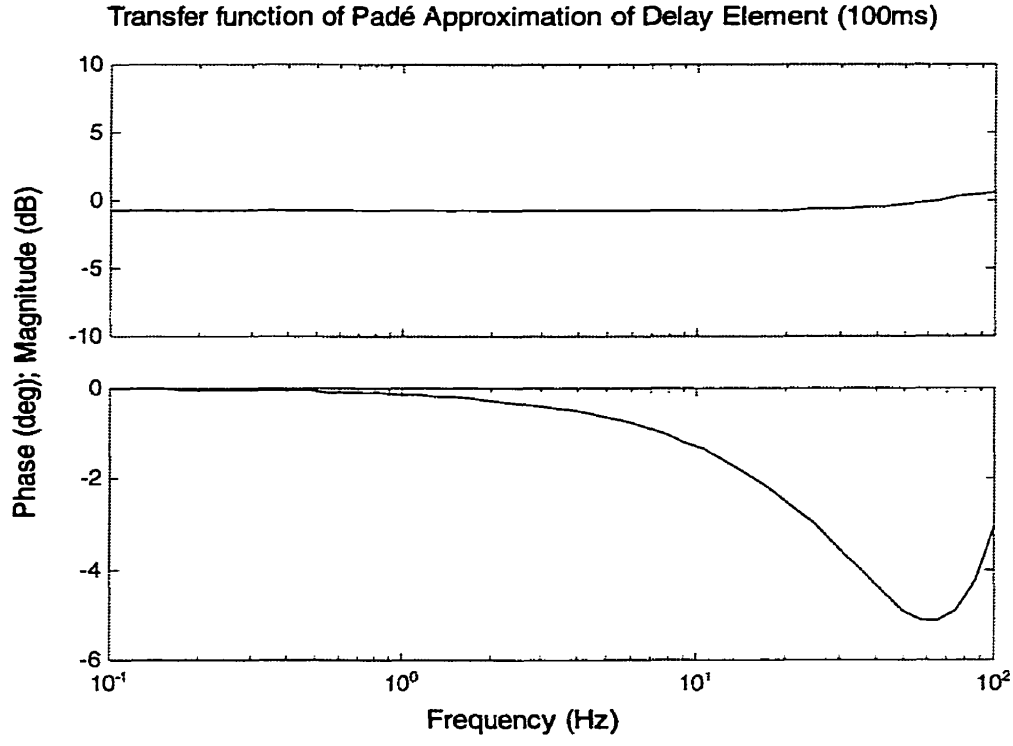

• Figure 27: Frequency Response of First Order Padé Approximation of a Delay Element

The transmission delay issue described above contributes the major discomfort factor in VE. Classical control theory proposes several alternative controllers one of which is the Proportional Derivative (PD) controller.

5.5 Proportional Derivative Controller

To compensate at least for transmission delays in Telepresence, an alternative to the proportional controller will be presented. The proposed controller is based on the classic Proportional Derivative (PD) scheme.

5.5.1 Description

The PD controller is nothing more than a predictive controller that is based on past inputs, and which attempts to predict the future input in order to compensate for system delays. The proposed controller is an extension to the proportional controller described in section 5.3 which relies directly on the past and present estimate of head rotation. The PD controller will be analyzed and its input will be in terms of the rotation angles of the head as produced by the velocity integrator.

When designing a predictive controller, one must look at the number of past input points used. A large number of points will produce a more accurate but sluggish response. A small number of sampled input points will be more sensitive to sensor noise and may not be as accurate. Another factor in the design of a PD controller is the gain associated with the differential part of the controller. A large gain will result in the output overshooting the desired trajectory for high-frequency input, while small gains will be insignificant compared to the proportional component.

5.5.2 Function Analysis

In the time domain, the PD controller's output is described as a function of its input in the following manner:

$$\begin{aligned} y(t) &= x(t) + K \cdot \frac{dx(t)}{dt} dt \quad K = Gain\ Factor \\ y(t) &= x(t) + K \cdot dx(t) \end{aligned} \tag{8}$$

Or expressed in terms of sampled data:

$$y[i] = x[i] + K \cdot \Delta x[i] \quad K = Gain\ Factor$$
$$y[i] = x[i] + K \cdot (x[i] - x[i-1]) \tag{9}$$

The proposed controller uses three past input points to determine the output and is described next:

$$\begin{aligned} y[i] &= x[i] + K_1 \cdot (x[i] - x[i-1]) + K_2 \cdot (x[i] - x[i-2]) + K_2 \cdot (x[i] - x[i-3]) \\ &= (1 + K_1 + K_2 + K_3)x[i] - K_1 x[i-1] - K_2 x[i-2] - K_3 x[i-3] \end{aligned} \tag{10}$$

When examined in the frequency domain:

$$Y[z] = (1 + K_1 + K_2 + K_3)x[z] - K_1 x[z]z^{-1} - K_2 x[z]z^{-2} - K_3 x[z]z^{-3} \tag{11}$$

The transfer function of the system is as follows:

$$\begin{aligned} T[z] &= \frac{Y[z]}{X[z]} = (1 + K_1 + K_2 + K_3) - K_1 z^{-1} - K_2 z^{-2} - K_3 z^{-3} \\ T[z] &= \frac{(1 + K_1 + K_2 + K_3)z^3 - K_1 z^2 - K_2 z^1 - K_3}{z^3} \end{aligned} \tag{12}$$

The graphical representation of the proposed predictor is shown in the following figure.

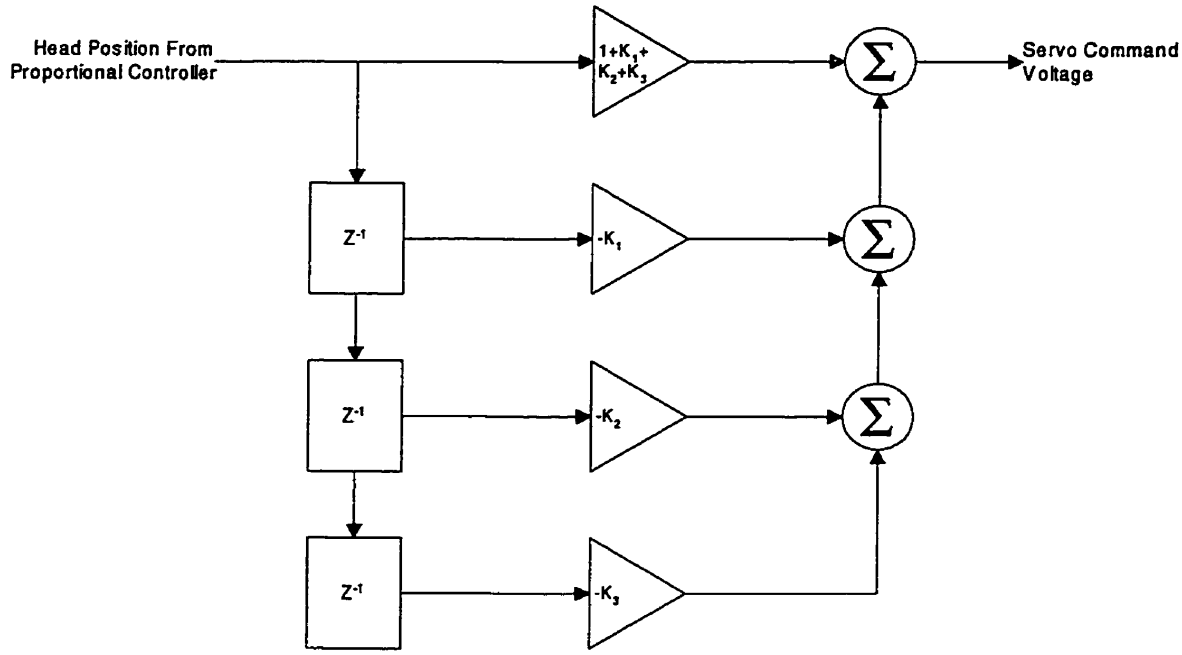

•Figure 28: Graphical Representation of Proportional Controller

The schematic describes a digital filter that uses the current sampled position along with three previous points to compute servomotor position command. The gains of the filters are $(1+K_1+K_2+K_3)$, $-K_1$, $-K_2$, and $-K_3$.

Figure 29 shows the step response of such a system while Figure 30 shows its frequency response, and demonstrates the sensitivity of the overshoot to the selected parameter set.

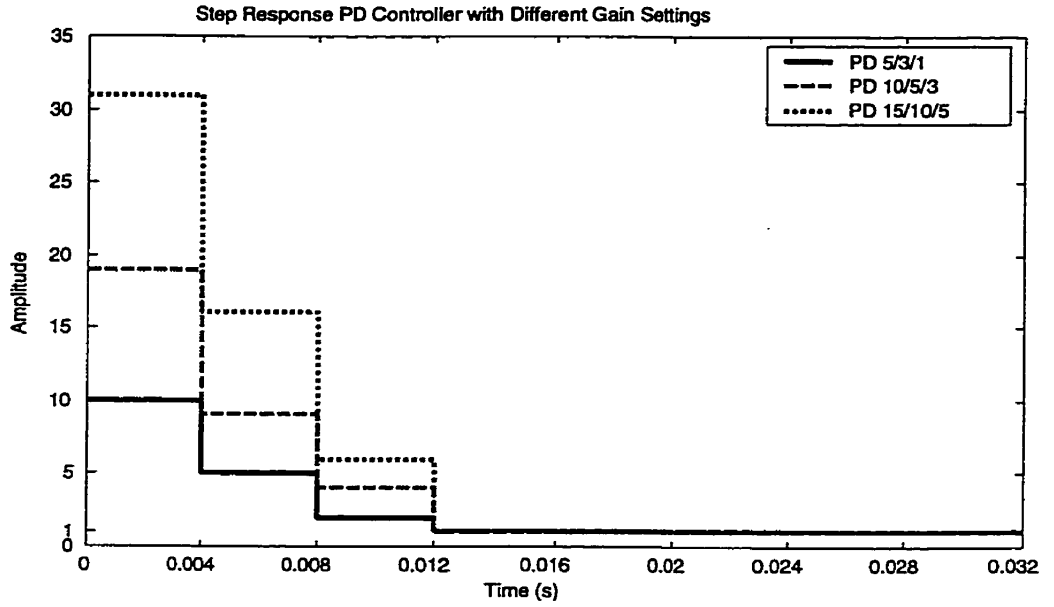

•Figure 29: PD Controller Step Response

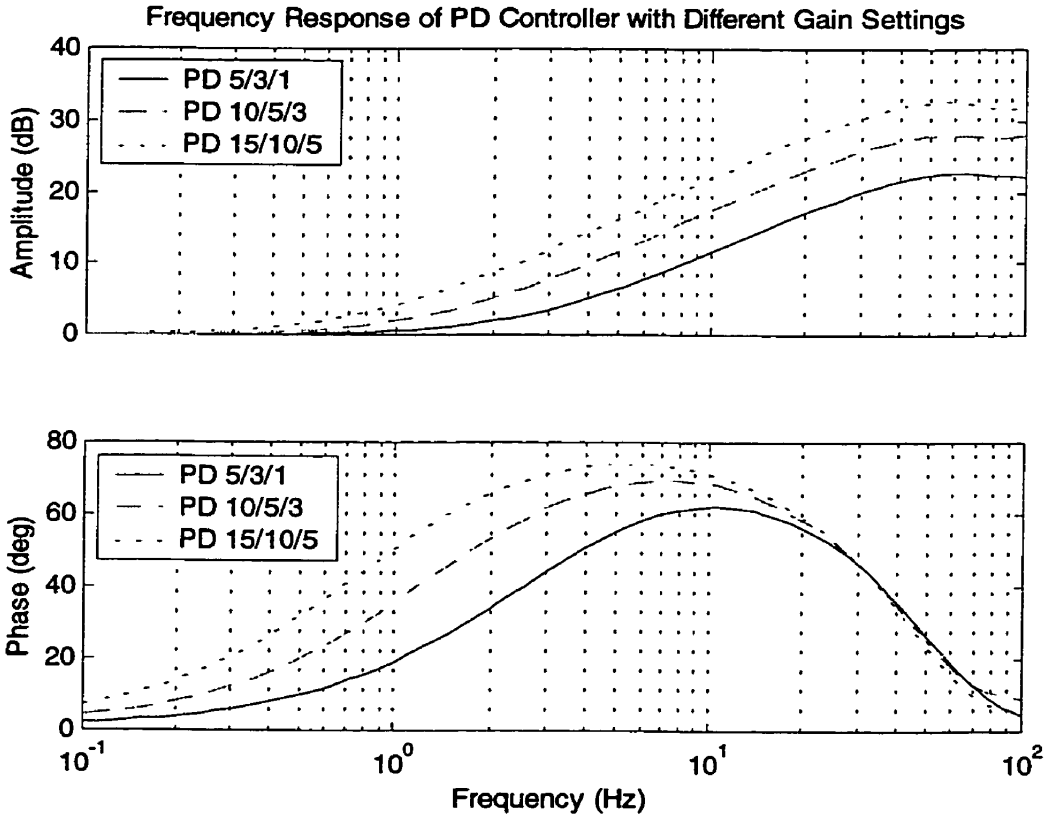

•Figure 30: PD Controller Frequency Response

5.5.3 Implementation

The proposed controller uses three previous input points produced by the velocity integrator to determine where the next input will be. Additions to input points will obviously produce a more accurate prediction, but at the expense of extra delay. The selection of the PD gains is a function of the expected overall delay time. A larger delay implies a larger gain set. The complete code section for the PD controller is described in Appendix B.

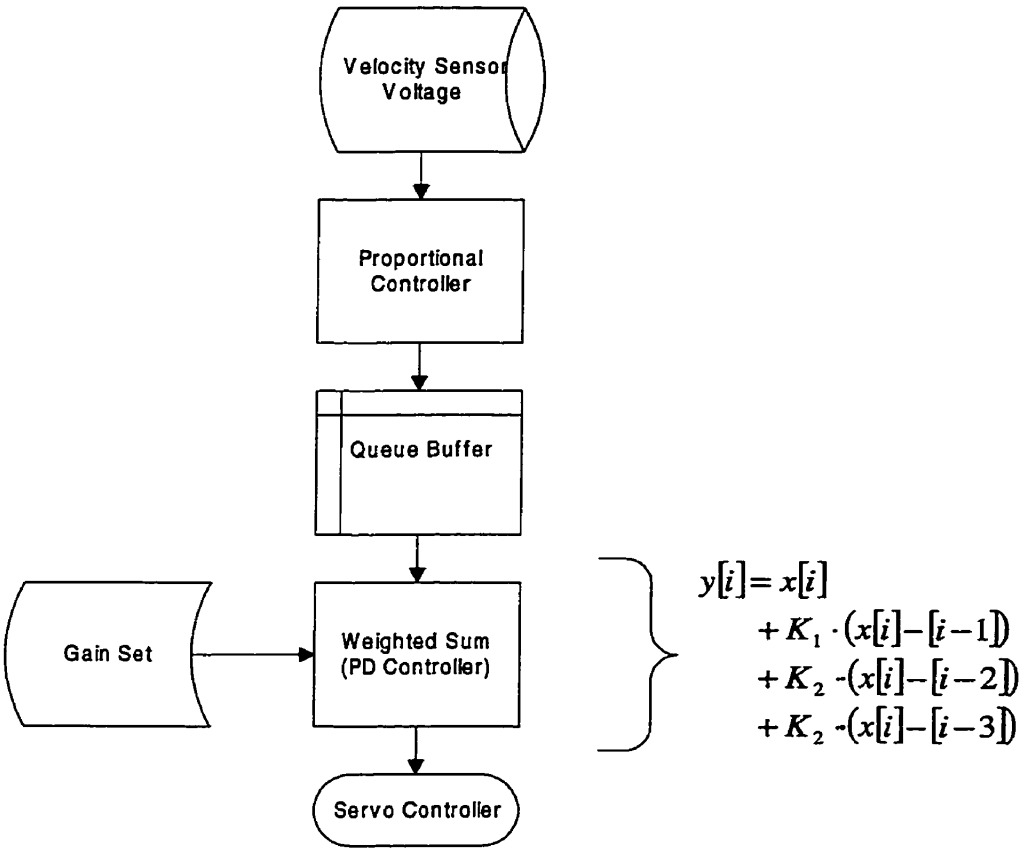

•Figure 31: Proportional Derivative Controller Code Flowchart

5.5.4 Known Limitations

Unfortunately, the PD controller is not the magical solution to all delay problems. It too has limitations and known problems:

1) The PD controller is highly sensitive to sensor noise. Any extraneous noise will be amplified by the derivative component of the controller. This can be observed as servomotor vibrations. Attempting to reduce the amount of sensory noise using lowpass filters increases the system phase lags, thereby contradicting the original objective. Fortunately, the Head velocity sensor used in this project does have a high Signal to Noise Ratio (SNR) and hence the amount of servomotor vibration is unnoticeable.

2) As seen in Figure 30, a PD controller with a fixed set of parameters only adds a constant phase lead over a certain range of frequencies. For different transport and reaction delays, different parameters set must be implemented. This process is more or less a manual process. The parameters of the PD controller must be manually adjusted in order to obtain a suitable frequency and step response, for each intended application and user.

3) From Figure 29, it is clear that the PD controller will cause the servomotors to overshoot their target considerably when attempting to compensate for large delays. The user of the VE system may or may not be able to tolerate this overshoot. Generally speaking, as long as the total number of points used in the PD controller is kept low, the servomotors will be driven fast enough back to the desired position. Moreover, the overshoots resulting from the use of the PD controller might not be as detectable thanks to the frequency response of the servomotors which behave as low pass filters.

4) The ability of the PD controller to cope with any type of servomotor is both an advantage and a disadvantage. On one hand, it is universal and is independent of the servomotor response. On the other hand, it does nothing to improve servomotor weaknesses, such as vibration and other mechanical limitations. This issue however is not of great importance since typical servomotors usually have good performance in the bandwidth of the human head.

Chapter 6 Experiments and Results

This chapter includes the results of different performance tests applied to both the Proportional Controller and the Proportional Derivative Controller. These include both objective and subjective measures of evaluation.

System identification was used to evaluate the results of experiments relying on MATLAB v5.3 with System Identification, Control, and Signal Processing toolkits. The Simulink tool in MATLAB provides a way of simulating the VE system with the software.

6.1 Simulation Results

In order to select the initial gain settings of the PD controller, simulation of the Virtual Environment is required. The human gaze controller within the VE system is presented with a 50 degrees spatial target. The VE system's parameters are set to simulate the desired environment, notably the system's total delay, and the resulting gaze shift is recorded. Ideally, the gaze controller's response with the VE system should be the same as that it would produce naturally. The PD controller's main objective is to bring back that response to the idealistic one or at least as close as possible.

The following figures describe the process. Note that Figure 32 represents the idealistic situation where the VE system's response is equivalent to an all pass filter with no phase lag, that is the human gaze controller in a natural context. Figure 33 shows the effect of the VE system with the simple proportional controller on the gaze shift. The ripple effect is due to the delay in the visual feedback: system poles are now complex. Figure 34 shows the PD controller with the ideal gain settings that bring back the gaze shift close to its original shape. Figure 35 shows the results of further increasing the PD controller gains. The overall system becomes over-damped. Figure 36 and Figure 37 show the simulation of the system with an additional 200 ms transmission and reception delay.

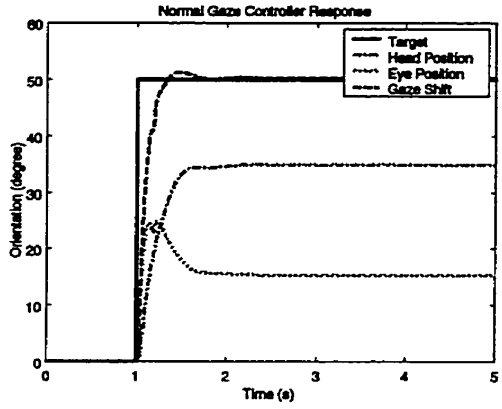

•Figure 32: Normal Gaze Controller Response

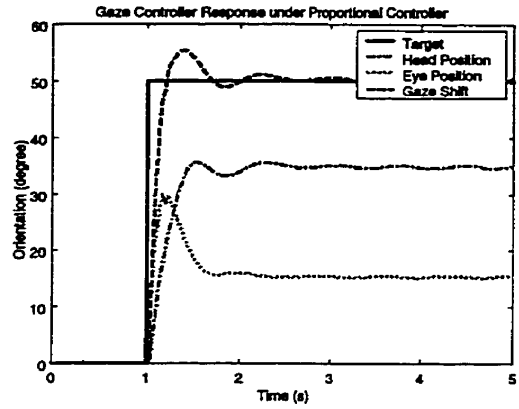

•Figure 33: Gaze Controller Response under Proportional Controller

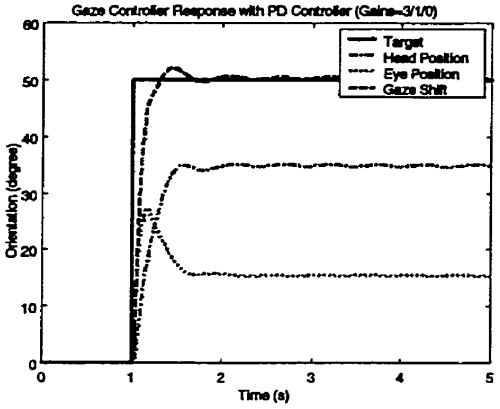

•Figure 34: Gaze Controller Response with PD Controller (Gains 3/1/0)

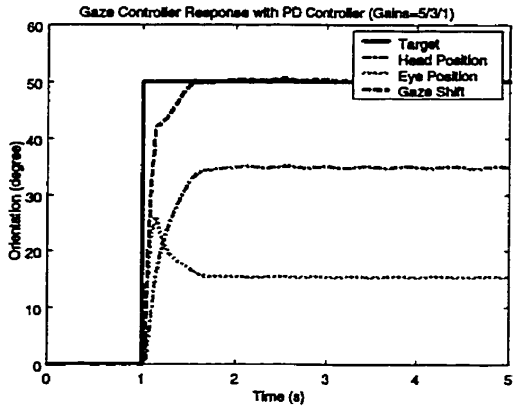

•Figure 35 : Gaze Controller Response with PD Controller (Gains 5/3/1)

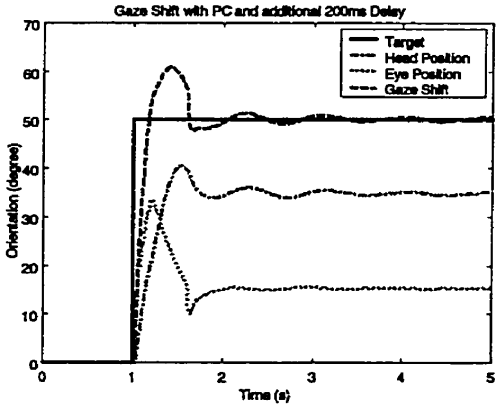

•Figure 36: Gaze Shift with PC and additional 200ms Delay

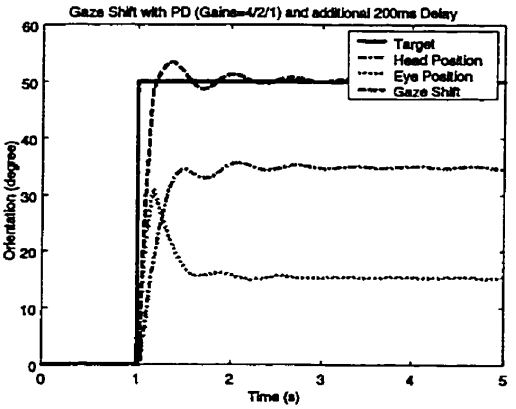

•Figure 37: Gaze Shift with PD (Gains=4/2/1) and additional 200ms Delay

Clearly the PD controller allows a return to near normal gaze trajectories. However the optimal parameter set is dependent on the delay to be compensated for and on the dynamics of the human operator.

6.2 Analysis Methodology

6.2.1 Statistical Analysis

Cross correlation techniques are primarily used to describe the sequential structure of a signal or signals. They provide a mean of deducing repeatability within a signal or determining similarity between two or more signals.

First start by defining the r^{th} moment of a signal about the origin:

$$\mu_r' = E\left[x^r\right] = \sum_x x^r . f(x) \text{ Where f(x) is the distribution of x} \tag{13}$$

μ_1' is called the Mean of the distribution of x, or simply the mean of x and is henceforth denoted by μ.

The r^{th} moment about the mean of the random variable x is defined as follows:

$$\mu_r = E\left[(x-\mu)^r\right] = \sum_x (x-\mu)^r . f(x) \tag{14}$$

The second moment about the mean of a random variable is indicative of the spread or dispersion of the distribution of that random variable and is usually known as the Variance of the distribution of x or simply the variance of x and is denoted as $\sigma^2 = \text{var}(x) = \mu_2$. The square root of the variance or σ is well known in statistics as the Standard Deviation of the distribution of the random signal x.

Since the mean of a sampled signal x will depend on the samples taken, it is safer to **estimate** the mean of a signal rather than to specify it. This implies that the true mean of a signal is usually within some interval $\hat{\mu}_1 < \mu < \hat{\mu}_2$ with a probability equal to $P(\hat{\mu}_1 < \mu < \hat{\mu}) = 1-\alpha$. Such an interval is called (1-α)*100% Confidence Interval, with the fraction 1-α called the Confidence Coefficient or the Degree of Confidence, and the $\hat{\mu}_1$ and $\hat{\mu}_2$ called the upper and lower confidence limits. The confidence interval for an estimated μ with a standard deviation σ can be computed using the following formula [7]:

$$\mu - t_{\alpha/2,n-1} \cdot \frac{\sigma}{\sqrt{n}} < \mu < \mu + t_{\alpha/2,n-1} \cdot \frac{\sigma}{\sqrt{n}} \tag{15}$$

Note that for n>30, $t_{\alpha/2,n-1}$ becomes practically independent from n. The t-function is a well-tabulated function.

The Auto-Correlation function of a signal x(t) is defined by the following equation:

$$R_{xx}[m] = E\{x[n]x[x+m]\} \tag{16}$$

The Auto-Covariance function is defined in a similar manner to the auto-correlation function but with the mean of the signal removed, which makes it a much better choice for analysis.

$$C_{xx}[m] = E\{(x[n]-\mu_x)(x[n+m]-\mu_x)\} \tag{17}$$

Note that for a zero mean signal, the auto-covariance and the auto-correlation functions are identical. The relation between the auto-covariance and the auto-correlation

functions is simply $C_{xx}[m] = R_{xx}[m] - \mu_x^2$. Note also that for the zero lag (m=0), the auto-covariance function is equivalent to the variance of the signal x.

The normalized version of the auto-correlation is known as the Auto-Correlation Coefficient Function (ACCF) and is defined as:

$$r_{xx}[m] = \frac{C_{xx}[m]}{C_{xx}[0]} \tag{18}$$

The ACCF is the most useful of all three correlation functions because it is mean and amplitude independent. The values of the ACCF are usually interpreted as the correlation within the signal itself. The values of the ACCF range from 1, representing a complete correlation to –1, representing a completely negative correlation, passing by 0 which represents no correlation.

While the auto-correlation functions are used to examine the relationships within a signal, the cross-correlation functions are used to determine the relationship between two signals. They follow the same definition [13]:

$$R_{xy}[m] = E\{x[n]y[x+m]\} \tag{19}$$

$$\begin{aligned} C_{xy}[m] &= E\{(x[n]-\mu_x)(y[n+m]-\mu_y)\} \\ C_{xy}[m] &= R_{xy}[m] - \mu_x\mu_y \end{aligned} \tag{20}$$

$$r_{xy}[m] = \frac{C_{xy}[m]}{\sqrt{C_{xx}[0]C_{yy}[0]}} \tag{21}$$

The last function is the Cross-Correlation Coefficient Function (CCCF), which is the representation of the correlation between the two signals x and y with the same interpretation of that of ACCF. The value of the CCCF at zero lag (m=0) will be unity only if the two signals x and y are identical to within a scale factor. The unity value of the CCCF at a lag position different than zero represents the time displacement between the two signals: positive lag represents a delay and negative lag represents a predictive system.

The mean estimate and confidence intervals will be used primarily to examine the performance of subjects under different controller configurations, whereas the correlation techniques will be used to evaluate the system performance using different controller configurations but with no human interference.

6.2.2 Frequency Response Estimation

Given certain input and a resulting output, system identification can be used to determine the governing dynamic relationship. The MATLAB identification toolkit is used to perform such a task. Several options are implemented in this toolkit, including the ARX parametric model, spectral model based on the Blackman-Tukey or the Smoothed Fourier Transform, or a correlation model. The ARX parametric model is used since it is quite flexible and is very suitable for linear system modeling.

The ARX model is a linear difference equation that relates the input x[n] to the output y[n] in the presence of white noise W[n] as follows:

$$y[n]+a_1 y[n-1]+\ldots+a_{n_a} y[n-n_a]=b_1 x[n-n_k]+\ldots+a_{n_b} x[n-n_k-n_b+1]+W[n]$$

(22)

The size of the difference equation is thus determined by the three parameters: n_a, n_b, and n_k. Note that n_a is the number of poles, n_b+1 is the number of zeros, and n_k is the pure time delay (the dead time) in the system. For a sampled data control system, typically n_k=1 if there is no dead time [12].

System identification comes into play in an attempt to determine the two arrays of coefficients a_i and b_i for a given n_a, n_b, and n_k. There are two methods to estimate the coefficients a_i and b_i: Least Squares (LS) and Instrumental Variables (IV). [12]

In the least squares method, the sum of the squares of the Right Hand Side (RHS) of the difference equation minus the sum of that of the Left Hand Side (LHS) is brought to a minimum with respect to a_i and b_i.

For the IV method, coefficients a_i and b_i are computed so that the errors (RHS-LHS) become uncorrelated to certain linear combinations of the inputs.

6.3 System Identification

In order to best estimate a system response, the input signal to that system is chosen to be a band limited white noise with spectral content that covers the range of frequencies of interest. The response of the system is then measured and the system model and performance are determined using the variety of analysis techniques available.

6.3.1 Head Sensor Performance

In order to measure the head performance, a calibration is performed by using known motions and comparing to the sensor's output for linearity and bandwidth. No calibration set-

up with an independent speed transducer was available. Hence the manufacturer specifications were relied upon for the head sensor properties (section 4.3).

The specification indicates that the head sensor has a flat frequency response from DC up to 8 Hz and with an additional bias at DC. Since no correction for sensor dynamics was applied, this implies that all analysis data recorded with the velocity sensor are valid up to 8 Hz. The DC bias component is always taken care of by taking a reasonable average at the beginning of each experience and then subtracting it from the output of the sensor in software control. This does not reduce the DC bias of the sensor by 100% but is fairly accurate. MATLAB function detrend(.) takes care of removing any linear trend present in the output of the integration of the velocity sensor, remembering that $\int Constant \cdot dt = \text{Constant} \times t$

6.3.2 Servo Performance

Using band-limited white noise as servo commands, the response of the servomotors is then measured using the velocity sensor. Integrating the sensor velocity output produces the servo motor position response that is used along with the input to compute the frequency response of the servomotors-sensor cascade.

The results of this analysis are shown in the following figure.

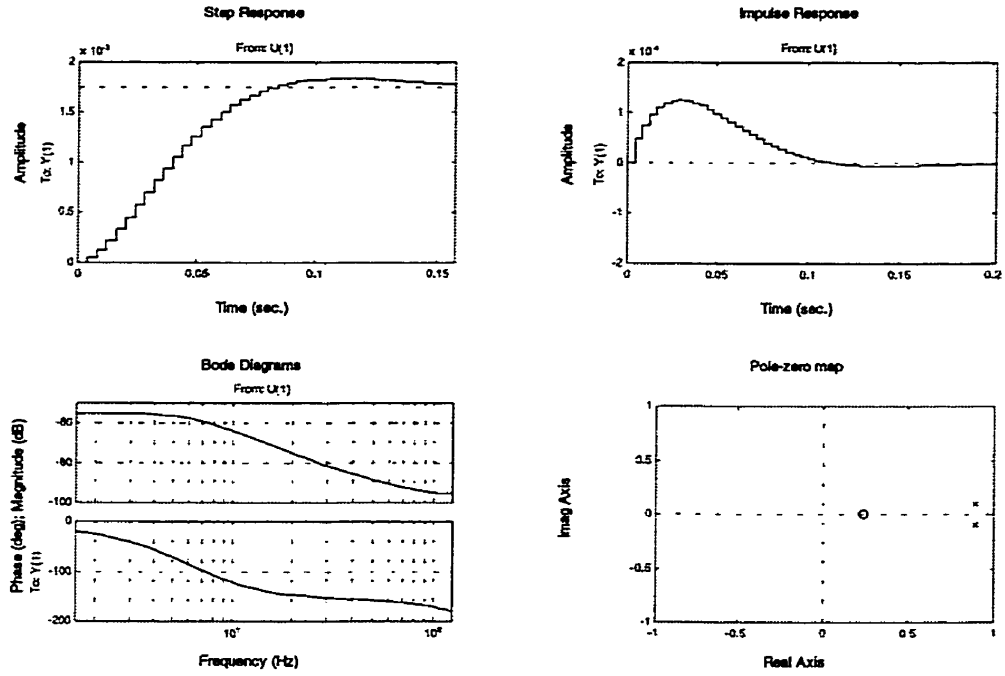

•Figure 38: System Analysis of the Head Servomotor

The response of the head tracker cannot be easily subtracted from the response of the servomotors. However, the cascade is relevant as it will be present in series with any controller to compensate for delays. The overall system performance will be examined in the next section.

6.4 System Performance

From section 5.1, it is clear that the system to be studied comprises the following subsystems:

- Head Tracker
- Host Computer
- Transmission delays

- Robotic Head
- Reception Delays

By summing the transmission and reception delays into one single delay element, the overall transfer function of the system is as follows:

$$T[z] = \text{HeadTracker} \times \text{Host Computer} \times \text{Delays} \times \text{Robotic Head} \tag{23}$$

Assuming that all systems are linear systems, this model can be rearranged into the following equivalent form:

$$T[z] = \text{Host Computer} \times \text{Delays} \times \text{Robotic Head} \times \text{HeadTracker} \tag{24}$$

The preceding form describes the following physical system: Drive the robotic head with a known signal computed by the host computer, and measure its response using the velocity sensor. The known signal can be anything from a band limited white noise (similar to that in the system identification) to recorded head movements. Here we decided to use head velocities recorded for 20 seconds from a human subject during natural randomized gaze shifts. These were then used as input to the subsystem simulations described above. The measured sensor results will help model the system as long as the head velocity recordings have enough spectral content over the frequency range of interest (i.e., 0-8 Hz).

In the following figures, the recorded head movement is shown both in time as well as in frequency domain and shows sufficient bandwidth for use as an input in the simulation studies.

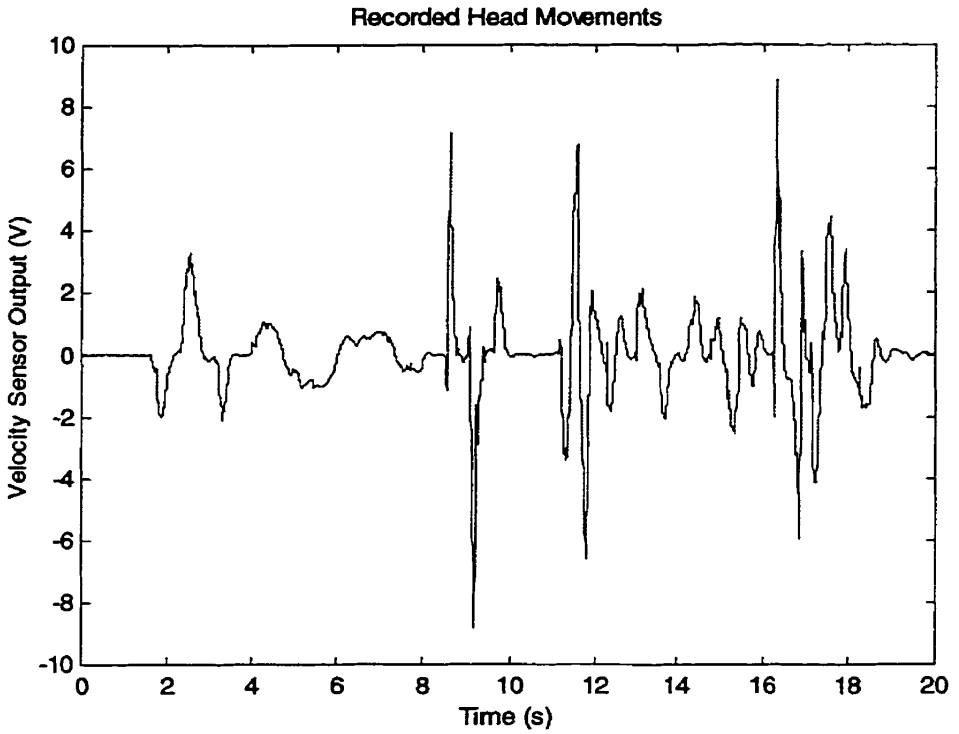

Figure 39: Recorded Head Movements

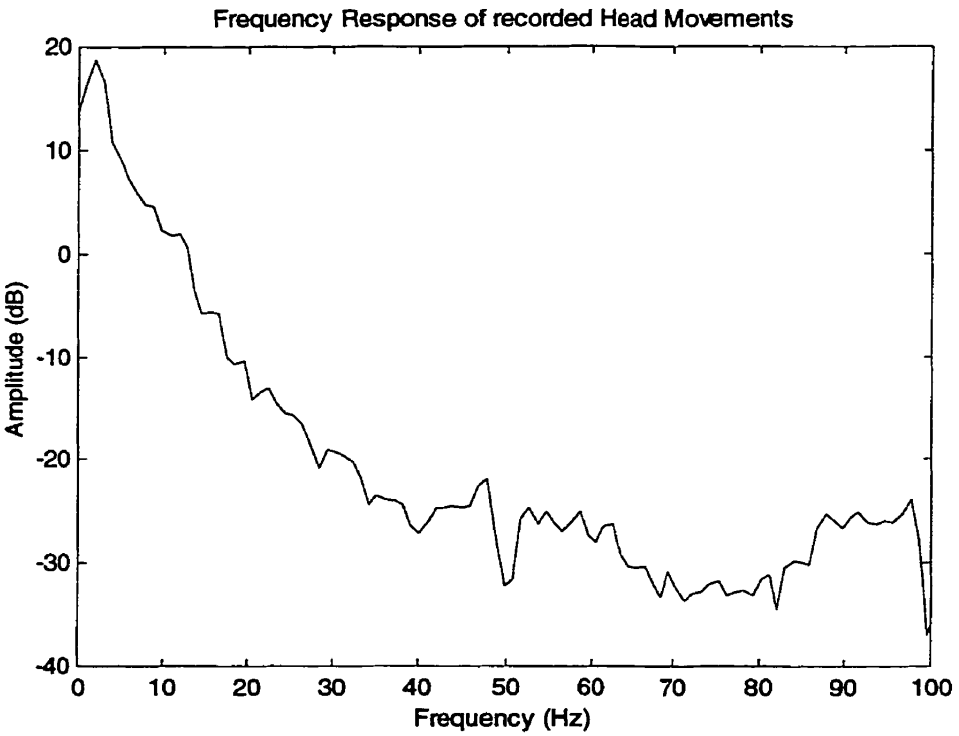

Figure 40: Frequency Response of Record Head Movements

In order to evaluate the different controllers under different operation conditions, additional delays are implemented via host software. The results of the host controller are stored in a queue buffer where it is delayed by the desired amount of points, thus effectively increasing the transmission delay. The total delay is equivalent to the number of points divided by the sampling rate. In practice, the transmission and reception delays are linearly proportional to the distance between the operating location and the remote operating location. A Telepresence operation on the moon might involve something in the order of half a second of total delay.

Next are the results of the comparison of the two software controllers (PC and PD) using a variety of total delays.

6.4.1 With no Delay

With the system running at its maximum efficiency, with no additional delays implemented, the actual system response can be obtained. The stored head velocity profiles were used as the input, and servo position (as determined by monitoring the head tracker mounted on the robot) was measured output.

In Figure 41 and Figure 42, the PC controller is compared against a PD controller with gain set of 5, 3 and 1, and also against a PD controller with gain set of 5, 5 and 5 (refer to equation 10 on page 55).

With the results of applying the CCCF to the servo position versus the input to the system, the following figure compaces overall performance delays with alternate controllers

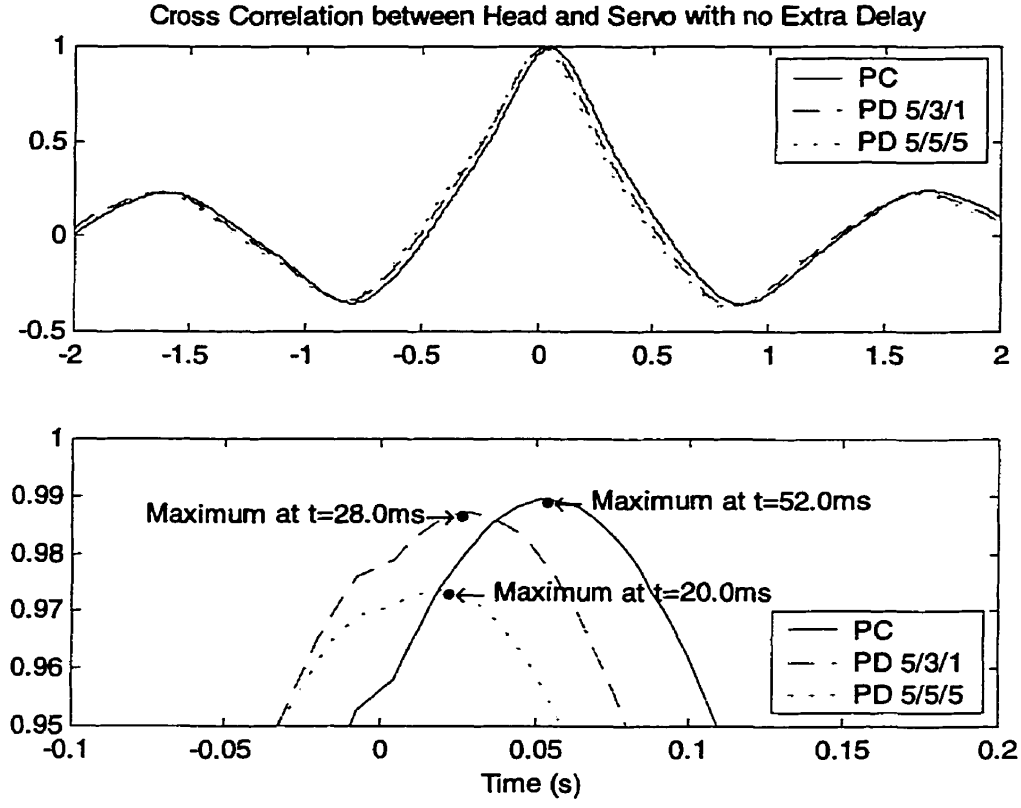

Figure 41: Cross Correlation between Head and Servo Reaction at Maximum System Performance. Lower Graph Zooms in Around Peak Near Zero Delay

From Figure 34, it is clear that the PD system outperforms the PC controller by 24 ms using the 5/3/1 gain set and by 32ms using the 5/5/5 gain set. Interestingly, the amount of correlation between the input and the output of the system declines as the gain of the PD controller is increased further, and the system becomes underdamped.

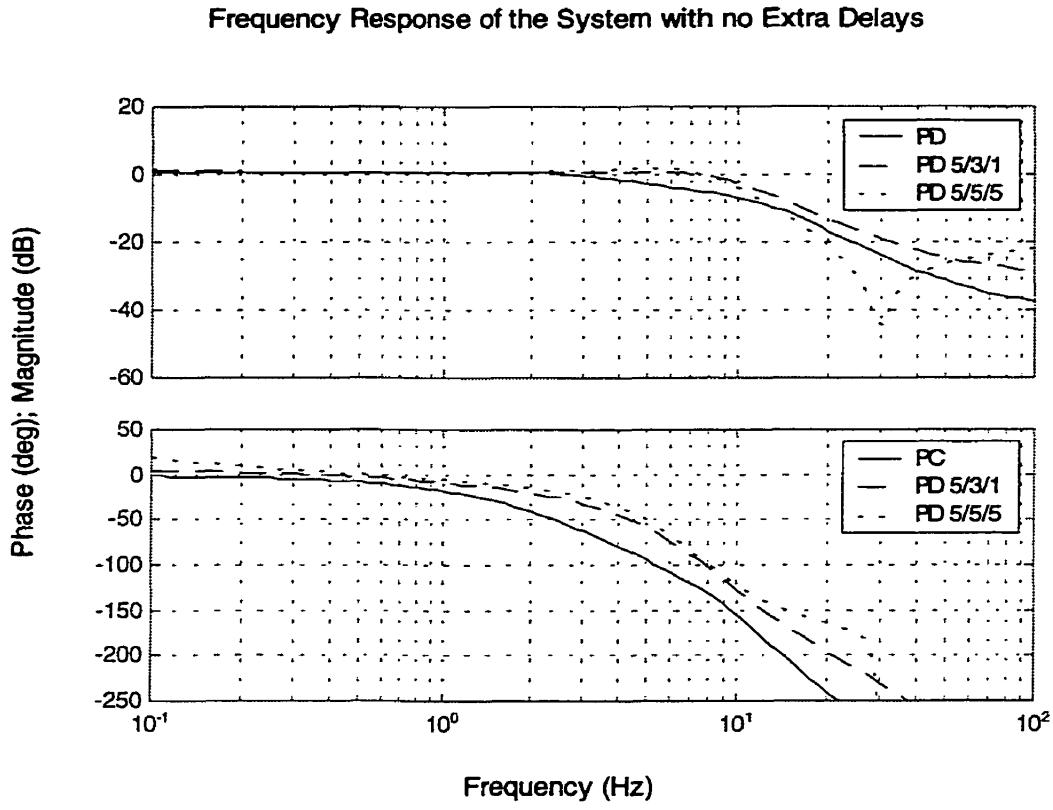

• Figure 42: Frequency Response of the System with no Extra Delays. Head Position Serves as Input While Servomotor Position Serves as Output

In Figure 42, the overall frequency response of the system is shown using the different controller strategies. It is clear that the PD controller has pushed the BW of the system from 2.5 Hz to 4.5 Hz with the gain set 5/3/1 and to 5.0 with the gain set 5/5/5. This increase in BW is a typical effect of a predictive controller.

6.4.2 With 200ms Extra Delay

Additional transmission and reception delays are implemented using a simple queue buffer located after the controller code. A 50-sample buffer is equivalent to a total delay of 50/250 = 200 ms.

As seen in Figure 43, similarly to the no extraneous delay case, there was a decrease in the overall system delay by 28 ms with the simple proportional controller. Using the PD controller with a higher gain factor decreased the total delay from 256 ms to 216 ms which is equivalent to a 40-ms improvement.

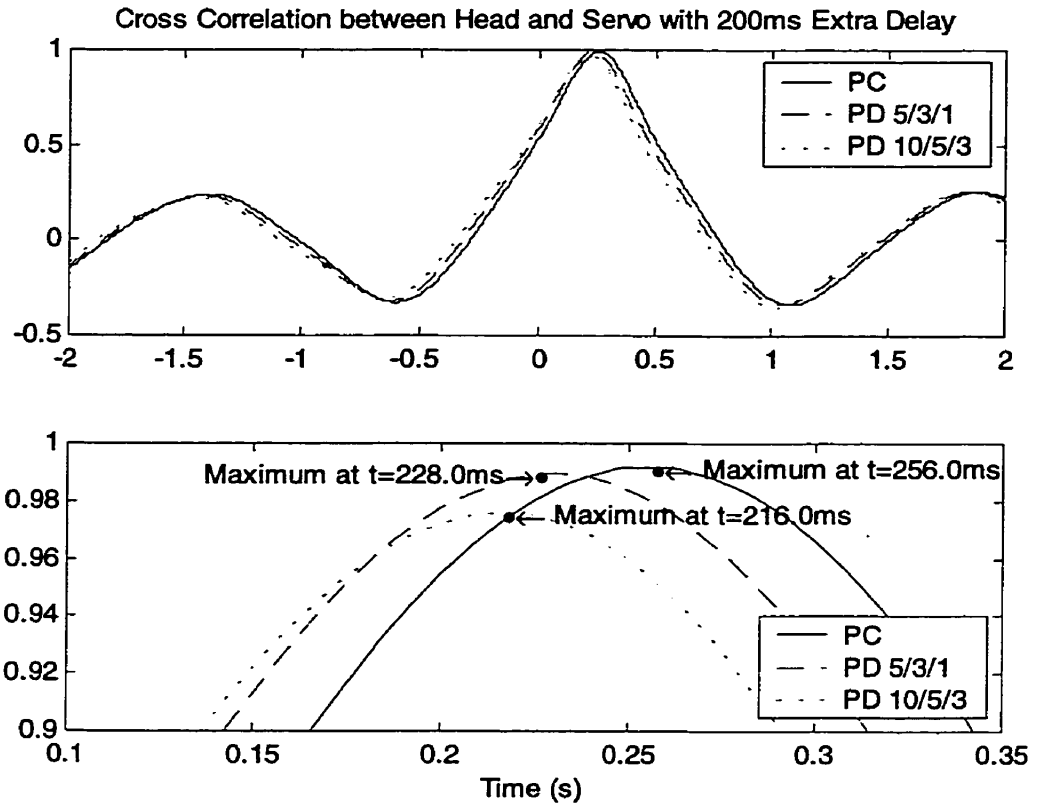

• Figure 43: Cross Correlation Between Head and Servo Reaction with 200ms Additional Delay

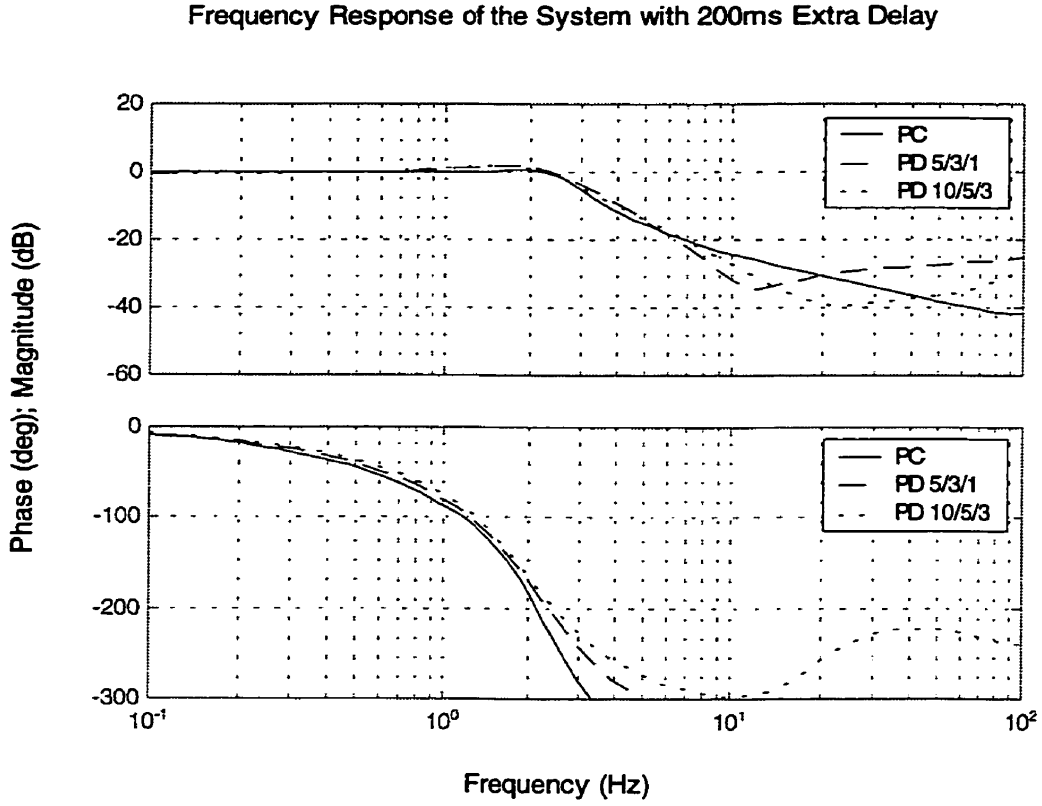

• Figure 44: Frequency Response of the System with 200 ms Extra Delay. Head Position Serves as Input While Servomotor Position Serves as Output

The BW improvement as seen in Figure 44 is an increase of 0.05 Hz in the case of a PD controller with a gain set 5/3/1 and an increase from 0.4 Hz to 0.5 Hz in the case of a PD controller with gain set 10/5/3. Although the absolute values of these increases are different from those of the previous case (no additional transmission delay), they are equivalent in the logarithmic sense, since the entire system is shifted back in frequency.

6.4.3 With 400ms Extra Delay

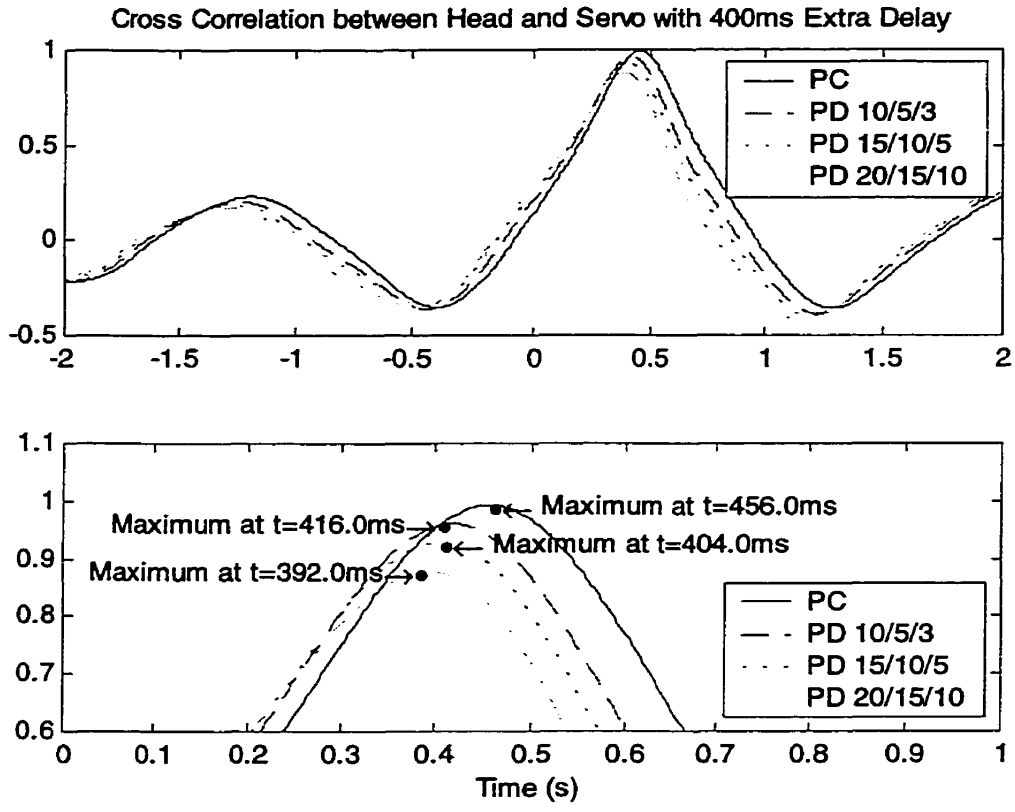

• Figure 45: Cross Correlation between Head and Servo Reaction with 200ms additional delay

The system performance, when using a 400-ms extra transmission delay, is only examined in time using the cross correlation coefficient function since the BW of the system is very low in the frequency domain. Similar to the previous cases, there was a total improvement of 40 ms with the gain set 10/5/3. The total delay dropped from 345 ms to 404 ms using the gain set 15/10/5 with the PD controller. The cross correlation coefficient, however, has also dropped from approximately 1.0 to about 0.93. This drop in correlation is obviously the side effect of overshooting when using large gain sets.

6.5 Human Subject Performance

In order to evaluate the system performance using human subjects, a measure of performance had to be developed.

In determining the side effects of Virtual Reality[15], McGee asked his subjects to perform certain visual tasks while immersed in the VR world (See attached Questionnaire in Appendix C). He measured the side effects of the VR on subjects using a questionnaire and then tabulated the results. This approach was considered for the evaluation of the different controllers. It proved to be impractical since it required the subjects to use the VE system for more than 10 minutes per system design. In order to properly assess the enhancement brought by the PD controller, at least 6 or 7 experiments had to be performed with extended delays between them.

An alternative measure was developed based on the assumption that the time needed to accomplish a visual task using the VE system is directly related to the total system delay. In other words, it will take a subject longer to perform in a system with larger time delays than it would in a fast system. This assumption makes it easy to measure the performance of a subject under a specific system.

6.5.1 Task Description

In typical "Point and Shoot" action computer games (i.e., Doom, Quake and Heretic), the player is usually on the lookout for targets. Once a target is identified, the player shoots it immediately. If the target happens to move in one direction or another, the player will follow it, and once in range, will shoot it down.

Similar to action games, the subjects here are presented with a visual target seen through the VE system. The target can be in the form of a circle or a square. The subjects identify the object by pressing on one of two button made accessible to them. Whether or not the subject's choice is correct, the target moves to another location, leaving behind a short but visible trace to indicate its motion direction. The target's movements are computed as to always position the target outside the field of view of the cameras. In this manner, subjects are forced to follow the target using their head and not their eyes.

The size of the jump between two consecutive target locations is random, as well the direction of the jump and the shape of the target (two). The distance between consecutive targets, the time required to identify targets (button press) as well as the correctness of the identification are stored in a file for post processing. The distance between the robotic head and the projection screen that is used to project the targets is used to compute the angular rotation required to center the cameras on the targets. Angular speed of the response is calculated as angle between targets divided by the time required for identification. For each experiment, the subject is presented with 50 randomized horizontal targets. Average time required for data acquisition in each experiment is roughly one to two minutes. The mean and confidence intervals are computed for each experiment and results of an entire session comparing various controllers are plotted together.

A sample figure below shows the results of such a session. The subject performed a total of 13 experiments with two software controllers and with different settings for the PD controller. An increase in the angular speed measure is equivalent to a reduction of the time required to perform the task and hence equivalent to a reduction in the overall system delay

and/or an increase in system bandwidth. Hence increases in measured average speeds are desirable.

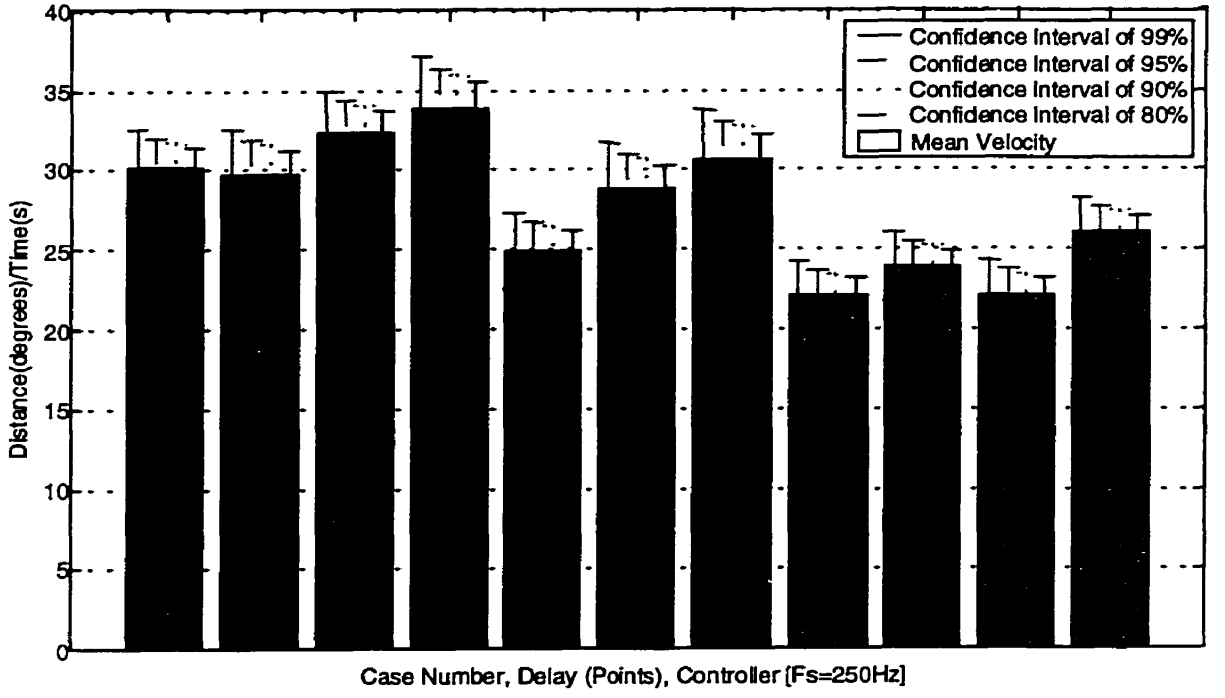

Figure 46: Performance Evaluation of Subject

6.5.2 Results

Nine subjects participated in this experiment. None were paid for their participation. Their physical condition and their total comfort was assessed using the Motion Sickness History Questionnaire (MSHQ) found in Appendix C. This questionnaire was adapted from the Motion History Questionnaire of the Essex Corporation. All subjects were males, ranging in age from 16 to 60 years old. The average age is 32 years with a standard deviation of 17 years.

The MSHQ was used to assess the physical condition of subjects. Most subjects were in good physical condition and had a good night sleep before performing the experiment. From their MSHQ, most subjects indicated that they are not **very** susceptible to motion sickness. Subject #5 had an ear surgery that resulted in increased sensitivity to motion sickness. He had a moderate headache and eye strain symptoms after the experiment.

Surprisingly, most of the subjects who had some pre-experiment symptoms such as headaches, general fatigue and drowsiness came out with no post-experiment symptoms! The consensus was that having to concentrate on the experimental task resulted in them forgetting about their previous symptoms.

Due to problems with the head tracker, the results of one experiment had to be discarded. The head tracker had received a physical shock and its output was highly contaminated with noise. The experiment did however demonstrate the susceptibility of the PD controller to sensor noise and how impractical the controller becomes with high gains in such conditions.

Tabulated results for all subjects are presented below

		0 Delay				200ms Delay				400ms Delay			
		80%	90%	95%	99%	80%	90%	95%	99%	80%	90%	95%	99%
1	PD 5/3/1	Same	Same	Same	Same	Same	Same	Same	Same	***Better***	***Better***	***Better***	Same
	PD 10/5/3	Same	Same	Same	Same	Same	Same	Same	Same	***Better***	***Better***	***Better***	Same
	PD 15/10/5	N/A	N/A	N/A	N/A	***Better***	Same	Same	Same	***Better***	***Better***	***Better***	Same
2	PD 5/3/1	Same	Same	Same	Same	***Better***	***Better***	Same	Same	Same	Same	Same	Same
	PD 10/5/3	***Better***	***Better***	***Better***	Same	***Better***	***Better***	***Better***	Same	***Better***	Same	Same	Same
	PD 15/10/5	N/A	N/A	N/A	N/A	***Better***	***Better***	Same	Same	Same	Same	Same	Same
3	PD 5/3/1	Same	Same	Same	Same	Same	Same	Same	Same	***Better***	Same	Same	Same
	PD 10/5/3	***Better***	***Better***	Same	Same	Same	Same	Same	Same	Same	Same	Same	Same
	PD 15/10/5	Same	Same	Same	Same	***Better***	Same	Same	Same	Same	Same	Same	Same
4	PD 5/3/1	***Better***	Same	Same	Same	***Better***	***Better***	***Better***	Same	***Better***	Same	Same	Same
	PD 10/5/3	***Better***	***Better***	***Better***	Same	***Better***	***Better***	***Better***	***Better***	Same	Same	Same	Same
	PD 15/10/5	N/A	N/A	N/A	N/A	N/A	N/A	N/A	N/A	***Better***	***Better***	***Better***	***Better***
5	PD 5/3/1	***Better***	Same	Same	Same	Same	Same	Same	Same	Same	Same	Same	Same
	PD 10/5/3	***Better***	***Better***	Same	Same	***Better***	Same	Same	Same	Same	Same	Same	Same
	PD 15/10/5	N/A	N/A	N/A	N/A	Same	Same	Same	Same	Same	Same	Same	Same
6	PD 5/3/1	***Better***	***Better***	Same	Same	Same	Same	Same	Same	***Better***	***Better***	Same	Same
	PD 10/5/3	***Better***	***Better***	***Better***	Same	Same	Same	Same	Same	Same	Same	Same	Same
	PD 15/10/5	N/A	N/A	N/A	N/A	Same	Same	Same	Same	***Better***	***Better***	***Better***	Same
7	PD 5/3/1	Same	Same	Same	Same	Same	Same	Same	Same	Same	Same	Same	Same
	PD 10/5/3	Same	Same	Same	Same	***Better***	***Better***	***Better***	Same	***Better***	***Better***	Same	Same
	PD 15/10/5	N/A	N/A	N/A	N/A	N/A	N/A	N/A	N/A	Same	Same	Same	Same
8	PD 5/3/1	***Better***	***Better***	Same	Same	***Better***	***Better***	Same	Same	Same	Same	Same	Same
	PD 10/5/3	Same	Same	Same	Same	***Better***	Same	Same	Same	Same	Same	Same	Same
	PD 15/10/5	Same	Same	Same	Same	Same	Same	Same	Same	***Better***	Same	Same	Same
PD Improvement		75%	75%	38%	0%	88%	50%	38%	13%	88%	50%	38%	13%

• Table 5: Results of Subjective Evaluation

An improvement is considered to be valid if a subject's performance using a PD controller is better than that with a PC controller with a certain confidence level. The

improvement rate is computed as the total number of improved cases at that confidence level over the total number of cases.

As seen in the last row of the preceding table, there is a notable improvement in the subjective quality of the VE system. With a confidence level of 95%, there was a 38% improvement rate for the 0 ms addition transmission delay, 38% improvement rate with 200 ms additional transmission delay and 38% improvement rate with 400 ms additional transmission delay. The same numbers rise to 75/88/88% respectively at an 80% confidence level – promising results for such a small subject pool.

Surprisingly, the amount of improvement seems to be the same regardless of the transmission delay. This can be traced back to the fact that the PD controller adds only a fixed phase lead with a certain gain factor set.

Also worth noting is the actual subjective feeling experienced while using the PD controller. Most subjects commented that they felt that the system with the PD controller is faster and it felt smoother than the PC controller. The common trend was that it was easier to cope with the overshoot caused by the large gain factor set used in the PD controller than with the extra delay using the PC controller.

6.6 Additional Findings

After examining the limitations of the PD controller, this section serves as an initial probe on possible use of deterministic properties in the human operator.

As an initial stage, recordings of some subjects' head velocity helped to prove that the physics of the human head can be represented using a two-pole system or two exponentials.

The exponentials have two different time constants. For a given subject, the rise time constant was not very correlated with the final head position. It was also evident that the peak head velocity is a function of the total head shift and occurs at relatively constant delay from the start of the gaze shift. The following figure shows the relation between the velocity and orientation of the human head for a typical subject in sensor units (i.e. Volts).

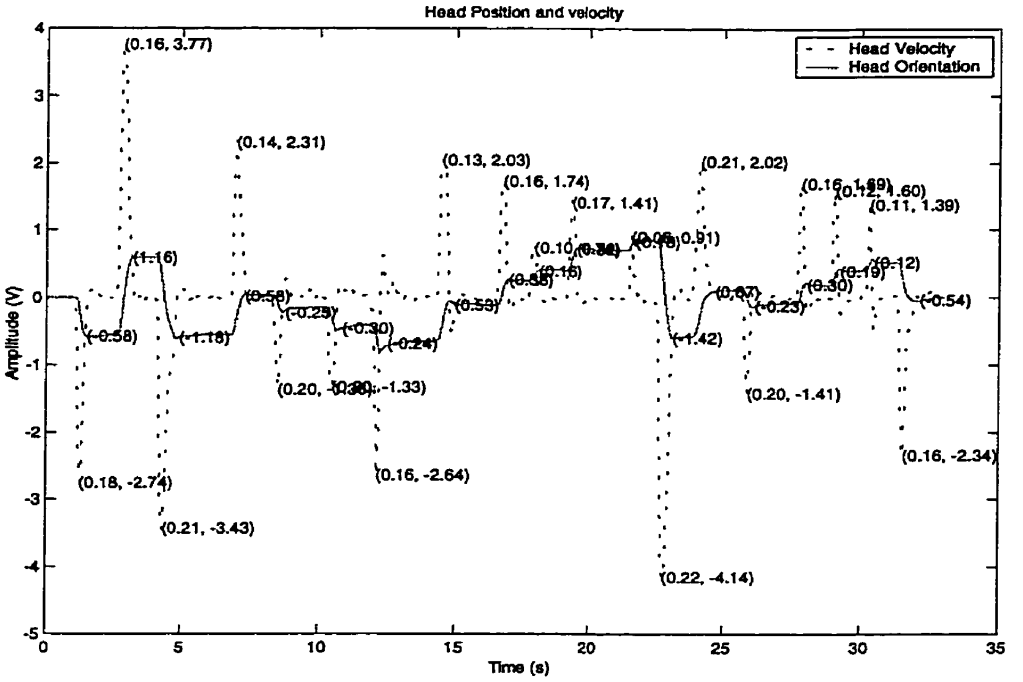

Figure 47: Relation between Head Position and Velocity (Sensor Units: Volts)

The peak velocity has a mean value of 157 ms with standard deviation of 43 ms. The following table shows the relation between all the different head variables.

Peak Time (ms)	Total Time (ms)	Peak Velocity(deg/s)	Total Rotation(deg)
180.26	445.36	-34.6680	-164.3760
159.06	562.00	69.3300	226.0200
212.08	848.30	-70.9800	-205.6440
137.85	477.17	34.6680	138.5280
201.47	466.57	-14.8560	-81.8400
203.53	563.61	-17.9220	-79.9800
156.56	532.30	-14.1180	-158.1840
125.25	626.23	32.0400	122.0340
156.56	407.05	22.8060	104.1120
99.04	284.75	9.3240	44.3820
173.32	383.79	19.4220	84.7740
61.90	210.47	7.7700	54.4800
222.85	557.11	-85.4520	-248.4780
197.20	443.69	-14.0700	-84.5340
160.22	382.07	17.8620	101.6580
123.25	308.12	11.3640	95.7060
110.92	308.12	7.0380	83.2560
160.22	764.14	-32.48	-140.28

• Table 6: Head Variables During Gaze Shifts

The relation between the head peak velocity and head final position can be better seen in Figure 48. Note that the data has been fitted with a second order polynomial in order to better assess the association between the two entities. The final position versus the peak velocity relation is a monotonically increasing function that can be very easily tabulated.

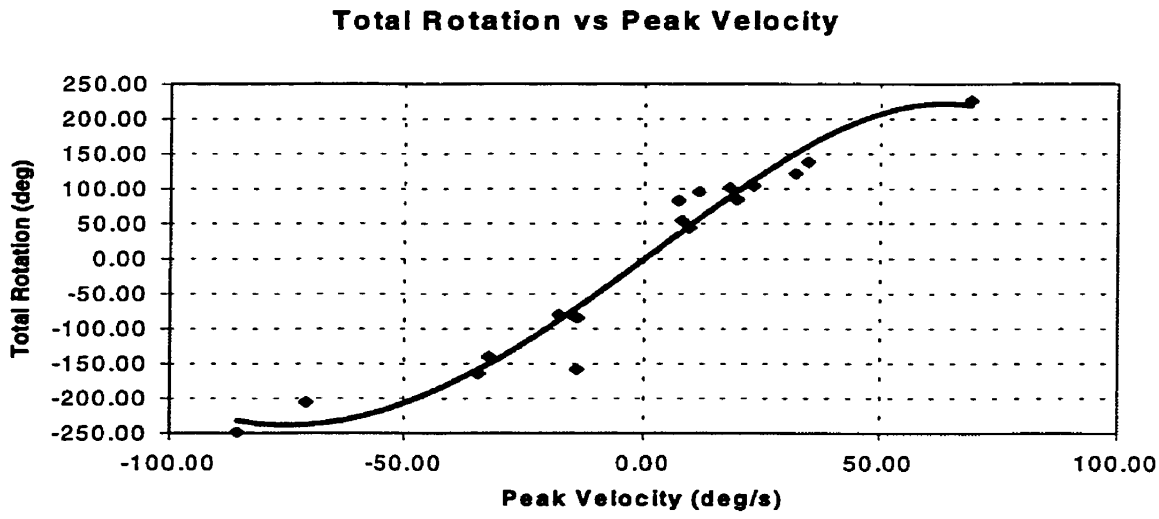

• Figure 48: Relation between Head Peak Velocity and Head Total Rotation

The process of acquiring such a function is also very simple and can be rendered fully automatic and part of a calibration process of the head sensor.

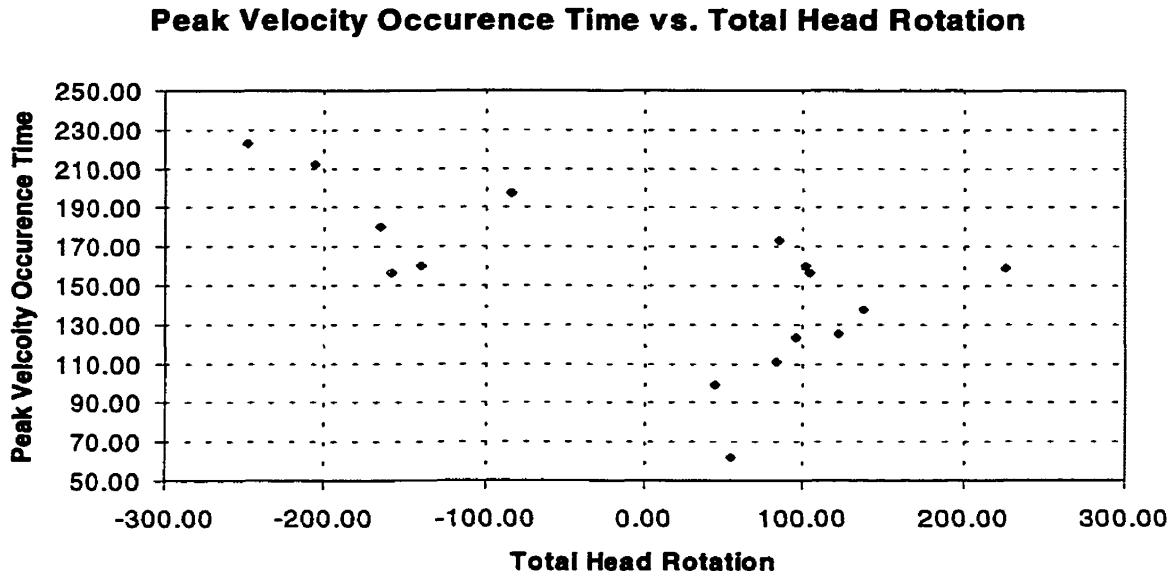

• Figure 49: Relation between the Peak Velocity Relative Occurring Time and Total Head Rotation

The time at which a peak velocity occurs with respect to the start of head movement is highly uncorrelated with the head's final position. This implies that if a certain minimum waiting time is applied after the start of movement of the user's head, then a peak velocity can be reliably detected.

These results indicate that human operator produces repeatable and consistent responses that can be used to design optimal controllers to compensate for both delays and dynamics. A brief description of such controllers is presented in the next chapter.

Chapter 7 Discussion and Conclusion

"Would you tell me, please, which way I ought to go from here?"

"That depends a good deal on where you want to get to", said the Cat.

"I don't much care where—", said Alice.

"Then it doesn't matter which way you go", said the Cat.

"— so long as I get SOMEWHERE", Alice added as an explanation.

"Oh, you're sure to do that", said the Cat, "if you only walk long enough."

Alice's Adventures in Wonderland, by Lewis Carroll

7.1 Conclusion

The main objective of this thesis was to determine the side effects of Virtual Reality and Telepresence. Once the causes of these effects were reviewed, suggestions for enhancements were presented. One of the main causes of discomfort in Virtual Environments is the time lag between head movements and the scene update resulting from such movements. The mismatch between what is expected and what is happening causes motion sickness to occur. One possible solution to such a problem is in the design of a better system controller.

In this thesis, an alternative to the traditional Proportional Controller is suggested. The proposed controller is based on the classical design Proportional Derivative strategy. At the heart of the PD controller is a predictive system that sums the position and the instantaneous velocity in an attempt to predict the future head position. This allows some anticipation in the update of scenes in the head-ups display.

The PD controller implemented in this thesis utilizes three past points in a first order linear interpolation with variable gains depending on the amount of prediction necessary. The PD controller adds a fixed phase lead to the system for a given set of gains. The phase lead comes however at the expense of overshooting the desired output during step responses (underdamped).

The Proportional Derivative controller was tested against the Proportional Controller using a home made Telepresence system. The Telepresence system consisted first of a head tracker used to measure the velocity of the user's head. The sensor's output is then integrated and passed through the software-base controller. The output of the controller is used to

control the remote servo motors which set the orientation of the miniature cameras whose output is fed back to the user via head mounted displays. Introducing adjustable buffer delay between the controller and servomotors can simulate the transmission distance between the user and the remote cameras. System performance was measured under different transmission delays up to 400 ms.

Two types of tests were applied to the controller: Objective and Experimental. The objective test comprised of injecting directly a known signal into the computer controller instead of the output of the sensor, and then measuring servomotor output using the actual head sensor, thus obtaining the response of the entire system. Statistical analysis demonstrated that the PD can decrease the response time of the system by at least 25 ms while frequency analysis showed that the BW of the system can be increased by at least 10% in all test conditions involving different transmission delays.

The experimental testing of the PD controller versus the Proportional Controller was done using human subjects. The subjects were asked to complete a remote visual task of identifying a random shape moving randomly to the right or left. The performance of the subjects was then measured by recording the time required to accomplish the visual task. Using the PD controller, subjects' performance went up by 38% with a confidence of 95% in all test conditions, or at least 77% at 80% confidence level. Most subjects commented throughout that the system felt smoother and faster than that with the Proportional controller and did not mind the overshoot as much as the delay.

It is certain that system delay is only one of many factors that cause user discomfort in a Virtual Environment. Video refresh speeds and video quality along with sensor noise

constitute other factors leading to Virtual Environments side effects. While technology might be able to correct for bad sensors or poor visual systems, smarter controllers can solve some more fundamental issues such as inherent system delays and slow response.

In this thesis, we have shown that simply by implementing a better controller than the traditionally used one, both significant objective and experimental improvements are achieved. Even smarter controllers based on a human head control models can be utilized. Such controllers will be user-dependant yet portable from one system to another.

7.2 Future Recommendations

7.2.1 Preliminary Human Response Prediction (Velocity versus Position)

Although Virtual Reality can benefit considerably from the addition of a simple PD controller, the PD controller does leave room for much more improvement. As discussed in section 6.6, an operator model-based controller would be a step forward. The strategy for such a controller is very simple and consists of the followings steps:

- Before VR use, perform a calibration process on the system operator. This includes asking the operator to look at different points in space and maintaining their head orientation at each new point for one second. Once the head velocity and position curves have been acquired, automatic local minimum and maximum peak detection can be applied to tabulate the peak velocity and head orientation shift. The operator's average time of peak velocity relative to the start of the gaze shift (T_v) can also be found in the same process. Compute a regression line to relate the expected size of a gaze shift to peak head velocity.

- During VR use,

    1) Maintain continuous update for HMD orientation based on the operator's orientation using a proportional controller.

    2) While head velocity increases, wait for at least T_v and look for the peak velocity amplitude. Based on the peak velocity amplitude, compute a projected head final orientation based on its current position, and the operator's regression line found during calibration.

    3) Using the projected head final orientation, compute an alternate camera system orientation trajectory based on the estimate of the total system delays and override the proportional controller output.

This strategy is largely based on the predictability of the movements of the human head as found in section 6.6. It has the advantages of simplicity (look-up table), stability despite variable operator characteristics and variable VR system delay.

7.2.2 More General Compensation for the Dynamics of both Operator and Servo Systems

Ultimately, a real head model can be developed from the calibration data and its transfer function can be computed. This transfer function along with the estimated hardware system dynamics can be incorporated in the system controller to produce any desired response from the total system. This will tune the system uniquely to each operator and can provide the best possible results.: i.e. an environments that feels "natural" and does not require user adaptation.

7.2.3 General Extension in Telepresence Properties

Improvements on the technological side of VE can yield a more "natural" feeling when immersed in such environments. Some of the suggestions that were presented in this thesis included higher resolution HMD for better quality video display and faster refresh rates for smoother video. Addition of a "distance cue" can improve the overall experience. This requires the addition of an auto-focusing camera system along with an automatically adjustable vergence-set-point.

7.2.4 Other Implications or Clinical Applications

From the examination of the side effects of Virtual Reality, adaptation to system performance can be used positively in clinical rehabilitation. The response of the system can be tuned to anything desired: for example, such a system can be used to force a certain adaptation of patients with Vestibulo-Oculo deficiencies.

Moreover, the use of the side effects of Virtual Reality can also be part of a controlled environment to test the susceptibility of people to motion sickness. (In NASA for instance, current methodology relies on the so-called "vomit-comet" where a particular subject is subjected to centrifugal forces and his performance in such an environment is then translated to susceptibility to motion sickness.) Why not use current VR systems that are also known to cause motion sickness?

Even after so many years of use of Virtual Environments, the world of possibilities is still largely uncharted and potential applications are limitless. Imagination is our guide in such a world.

ABBREVIATIONS

- A/D : Analog to Digital
- ACCF : Auto-Correlation Coefficient Function
- BW : Bandwidth
- CCCF : Cross-Correlation Coefficient Function
- D/A : Digital to Analog
- DC : Direct Current
- Deg : Degree
- DOF : Depth of Field
- EOG : Electro-Ocular Graph
- HMD : Head-Mounted Display
- I/O : Input/Output
- IV : Instrumental Variables
- LCD : Liquid Crystal Display
- LHS : Left Hand Side
- MS : Millisecond
- MSHQ : Motion Sickness History Questionnaire
- NVS : Night Vision System
- OKR : Optokinetic Reflex
- PC : Proportional Controller
- PID : Proportional Integral Derivative
- PD : Proportional Derivative
- PWM : Pulse Width Modulation
- RGB : Red Green Blue
- RHS : Right Hand Size
- Sec : Second
- SNR : Signal to Noise Ratio
- SSQ : Simulator Side-effects Questionnaire.
- VE : Virtual Environment
- VOR : Vestibular Ocular Reflex
- VR : Virtual Reality

REFERENCES

[1] Barnes G.R. and S.G Wells, "Modeling Prediction in Ocular Pursuit, The Importance of Short-Term Storage", *Current Oculomotor Research*, page 97-107. 1999.

[2] Bélanger Pierre, "Control Engineering", Saunders College Publishing.

[3] Breznen Boris, Shao-Ming Lu and James W. Gnadt, "Analysis of the step response of the saccadic feedback: system behavior", *Experimental Brain Research*, 111:337-344, Springer-Verlag 1996.

[4] Brittan D., "Knowing Where Your Head Is At". *Technology Review*, February/March 1995, 10-11.

[5] Collins C.J.S. and G.R. Barnes, "Independent Control of Head and Gaze movements during Head-Free pursuit in humans", *Journal of Physiology* 1999, pp. 299-314.

[6] Draper M., "Can Your Eyes Make You Sick? Investigating the Relationship Between the Vestibulo-Ocular Reflex and Virtual Reality", April 29, 1996 R-96-3. Seattle: University of Washington, Human Interface Technology Laboratory.

[7] Freund John E. and Ronald E. Walpole, "Mathematical Statics", Fourth Edition, Prentice Hall.

[8] Galiana H.L. and D. Guitton, "Central Organization and Modeling of Eye-Head Coordination during Orienting Gaze Shifts", In Sensing and Controlling Motion (eds Cohen, Tomko & Guedry) *Ann N.Y. Acad. Sci.* Vol 656, pp.452-471, 1992.

[9] Guedry FE. Rupert AR. Reschke MF. "Motion sickness and development of synergy within the spatial orientation system. A hypothetical unifying concept." [Review] [60 refs] *Brain Research Bulletin*. 47(5):475-80, 1998 Nov 15.

[10]Kawara Tetsuo., Masao Ohmi and Tatsuya Yoshizawa, "Effect on visual function during tasks of object handling in virtual environment with a head mounted display", *Ergonomics* 1996, vol. 39, No. 11, 1370-1380

[11]Komachi Y., K. Miyazaki, T. Murata, S. Nagata and K. Kani, "Stereopsis with normal and reversed binocular parallax using a head mounted display in normal and strabismic subjects", *Ergonomics*, 1996, vol. 39, no. 11, 1321-1329.

[12]Ljung Lennart, "System Identification Toolbox User's Guide", August 1995, The MathWorks Inc.

[13]Marmarelis P. Z. and V. Z. Marmarelis, "Analysis of Physiological Systems", Plenum Press, NY.

[14]Marran Lynn and Clifton Schor, "Multi-accommodative Stimuli in VR Systems: Problems and Solutions", *Human Factors*, 1997, 39(3), 382-388.

[15]McGee M. K., "Assessing Negative Side Effects in Virtual Environments", Master's Degree, Faculty of the Virginia Polytechnic Institute and State University, Blacksburg Virginia, 1998.

[16] Chaturvedi V. Gisbergen JA. "Shared target selection for combined version-vergence eye movements" *Journal of Neurophysiology*. 80(2):849-62, 1998 Aug.

[17]Merfeld DM. Effect of spaceflight on ability to sense and control roll tilt: human neurovestibular studies on SLS-2. Journal of Applied Physiology. 81(1):50-7, 1996 Jul.

[18]Oman CM. "Sensory conflict theory and space sickness: our changing perspective" Journal of Vestibular Research. 8(1):51-6, 1998 Jan-Feb.

[19]Palatsoukas D., "Gaze Control Fusing Eye-Head Coordination with Unified Saccadic and Smooth Pursuit Modes of Operation", Master's Degree, Faculty of Biomedical Engineering, McGill University, February 3rd, 1999.

[20]Proakis John G. and Dimitris G. Manolakis, "Digital Signal Processing Principles, Algorithms, and Applications", Second Edition, Macmillion.

[21]Richard C. Frecker and W. James MacLean, "Linear Multivariate Regression Technique for Calibrating 2-Dimensional Corneal-Reflection Eye Trackers", Proceedings of the 1989 Annual Conference of the Canadian Medical & Biological Engineering Society, June 1989, Toronto/Canada.

[22]Schilder P., P. Pasik and T. Pasik, "On-line analysis of Optokinetic Nystagmus by small general purpose digital computer", Acta Otolaryng 76: 443-449, 1973

APPENDIX A VISUAL BASIC CODE FOR HEAD TRACKER COMPENSATION

```
Private Sub System()
    Dim dSamplingRate As Double, dHeadGain As Double, iControllerType As Integer
    Dim dHeadBias As Double, iBiasMode As Integer
    Dim i As Long, iCounter As Long, iBiasCounter As Long, iRefreshEvery As Long
    Dim dStartTime As Double, dTotalTime As Double
    Dim Data As Variant, Data2 As Variant, bNulling As Boolean, dServoCmd As
Double
    Dim dHeadBuffer(0 To 10) As Double
    Dim dSamplingDelayBuffer(0 To 1000) As Double
    Dim dTransmissionDelayBuffer(0 To 1000) As Double

    ' Get Settings from Form
    dSamplingRate = cwnSamplingRate.Value
    dHeadGain = cwnHeadGain.Value
    iControllerType = cmbControllerType.ListIndex
    dHeadBias = cwnHeadBias.Value
    iBiasMode = cmbAutoBiasMode.ListIndex
    iRefreshEvery = cwnReferesh.Value

    bRunning = True

    ' Get bias on start (if requested)
    If iBiasMode = AutoBiasOnStart Or iBiasMode = AutoBiasOnStartOnNull Then
        txtInfo = "Biasing. Press Null when READY."

        iCounter = 0
        dStartTime = Timer
        dHeadBias = 0#
        Do
            DoEvents
            CWDIO.SingleRead Data2
            If Not bRunning Then
                txtInfo = ""
                Exit Sub
            End If
        Loop Until (Data2(0) And 2 ^ 2) > 0

        txtInfo = "Biasing... Release Null when DONE."
        Do
            Do
            Loop Until (i * 1 / dSamplingRate) <= (Timer() - dStartTime)
            CWAIPoint.SingleRead Data
            dHeadBias = dHeadBias + Data
            iCounter = iCounter + 1
            CWDIO.SingleRead Data2
            If Not bRunning Then
                txtInfo = ""
                Exit Sub
            End If
        Loop Until (Data2(0) And 2 ^ 2) = 0

        dHeadBias = dHeadBias / iCounter
        cwnHeadBias.Value = dHeadBias
        txtInfo = ""
    End If

    ' Start
    i = 0
    iBiasCounter = 0
    dStartTime = Timer
    iCounter = 0
```

```
dTotalTime = 0#

Do
    ' Synchronize sampling rate
    Do
        dTotalTime = Timer - dStartTime
    Loop Until (iCounter * 1 / dSamplingRate) <= dTotalTime

    ' Get status of nulling button
    CWDIO.SingleRead Data
    bNulling = ((Data(0) And 2 ^ 2) > 0)

    ' Emergency hardware Null button pressed
    If (Data(0) And 2) > 0 Then bRunning = False

    ' Move Head Buffer in time
    For i = UBound(dHeadBuffer) To LBound(dHeadBuffer) + 1 Step -1
        dHeadBuffer(i) = dHeadBuffer(i - 1)
    Next

    ' Read new head velocity
    CWAIPoint.SingleRead Data

    ' Compute bias if Null is pressed and as requested by user
    ' Null if nulling is performed by driving head buffer to 0
    If (iBiasMode = AutoBiasOnNull Or iBiasMode = AutoBiasOnStartOnNull) Then
        If bNulling Then
            If iBiasCounter = 0 Then
                dHeadBias = 0
                iBiasCounter = iBiasCounter + 1
            Else
                dHeadBias = (dHeadBias * (iBiasCounter - 1) + Data)
                dHeadBias = dHeadBias / iBiasCounter
                iBiasCounter = iBiasCounter + 1
            End If
            Data = -dHeadBuffer(0) * dSamplingRate + dHeadBias
            txtInfo = "Nulling/AutoBiasing"
        Else
            ' Process any head biasing computation if any
            If iBiasCounter > 0 Then
                iBiasCounter = 0
                cwnHeadBias.Value = dHeadBias
                txtInfo = ""
            End If
        End If
    Else
        If bNulling Then
            Data = -dHeadBuffer(0) * dSamplingRate + dHeadBias
        End If
    End If

    ' Additional Delay using buffer
    If cwnSamplingDelay.Value > 0 Then
        For i = 0 To cwnSamplingDelay.Value - 1
            dSamplingDelayBuffer(i) = IIf(bNulling, 0, dSamplingDelayBuffer(i
+ 1))
        Next
        dSamplingDelayBuffer(cwnSamplingDelay.Value) = Data
        If Not bNulling Then Data = dSamplingDelayBuffer(0)
    End If

    ' Get new head position into buffer using integral formula
    dHeadBuffer(0) = dHeadBuffer(0) + (Data - dHeadBias) * 1 / dSamplingRate

    ' Compute servo commands (Controller) [See Appendix B]
    dServoCmd = Controller(iControllerType, dHeadBuffer, dHeadGain)
```

```
        ' Additional Delay using delay
        If cwnTransmissionDelay.Value > 0 Then
            For i = 0 To cwnTransmissionDelay.Value - 1

dTransmissionDelayBuffer(i)=IIf(bNulling,0,dTransmissionDelayBuffer(i+1))
            Next
            dTransmissionDelayBuffer(cwnTransmissionDelay.Value) = dServoCmd
            If Not bNulling Then dServoCmd = dTransmissionDelayBuffer(0)
        End If

        ' Output servo commands
        CWAOPoint.SingleWrite dServoCmd, True

        ' Refresh indicators and wait for stop button
        iCounter = iCounter + 1
        If iCounter Mod iRefreshEvery = 0 Then
            txtCounter = iCounter
            txtSamplingRate = Format(txtCounter / dTotalTime, "0.000") & "Hz"
            txtNulling = IIf(bNulling, "Nulling", "")
            txtTotalTime = Format(dTotalTime, "0.00s")
            iBiasMode = cmbAutoBiasMode.ListIndex
            iControllerType = cmbControllerType.ListIndex
            DoEvents
        End If
    Loop While bRunning

    ' Done
    bRunning = False
End Sub
```

APPENDIX B VISUAL BASIC CODE FOR THE SOFTWARE CONTROLLER

The code presented below contains both Proportional Controller and PD controller code. The selection switch iControllerType determines at runtime which controller is active.

```
Public Function Controller( _
    iControllerType As Integer, _
    ByRef dHeadBuffer As Variant, _
    ByRef dHeadGain As Double) As Double

    Select Case iControllerType
    Case ControllerProportional
        Controller = dHeadBuffer(0) * dHeadGain
    Case ControllerPD
        ' Use dHeadBuffer with i = 0 for current point, i = 1 one point delayed
        Controller = dHeadGain * ( _
            dHeadBuffer(0) + _
            (dHeadBuffer(0) - dHeadBuffer(1)) * PDControllerGain(1) + _
            (dHeadBuffer(0) - dHeadBuffer(2)) * (1 / 2) * PDControllerGain(2) + _
            (dHeadBuffer(0) - dHeadBuffer(3)) * (1 / 3) * PDControllerGain(3))
    End Select
End Function
```

APPENDIX C MOTION SICKNESS HISTORY QUESTIONNAIRE -

MOTION SICKNESS HISTORY QUESTIONNAIRE

Date: _____

Subject: _____

Ported from M. K. McGee, "Assessing Negative Side Effects in Virtual Environments"

Motion History Questionnaire adapted from the Motion History Questionnaire of the Essex Corporation, 1040 Woodcock Road, Orlando, FL 32803

1) Date of birth _____

2) Gender M / F

3) Do you have any medical condition involving the heart or circulation? If yes, please provide the following information:

   Nature of condition:

   Major symptoms:

   Does this condition affect your day to day activities? Yes _____ No _____

4) 4. Are you in your usual state of fitness?

   Yes _____ No _____ If no, please indicate reason.

5) In general, how susceptible to motion sickness are you?

   Extremely_____ Very_____ Moderately_____ Minimally_____ Not at all_____

6) Have you been nauseated for any reason (including flu, alcohol, etc.) during the past eight weeks?

   Yes_____ No_____ If yes, under what conditions:

7) 7. Most people experience slight dizziness (not as a result of motion) three to five times a year. The past year you have been dizzy:

   Greater than 3-5 times_____ 3-5 times_____ Less than 3-5 times_____ Never dizzy_____

8) Have you ever had an ear illness or injury which was accompanied by dizziness and/or nausea?

   Yes_____ No_____ If yes, describe the illness:

9) From any experience in the air, how often would you say you get airsick?

   Always_____ Frequently_____ Sometimes_____ Rarely_____ Never_____

10) From any experience at sea, how often would you say you get seasick?

Always_____ Frequently_____ Sometimes_____ Rarely_____ Never_____

11) From any experience in cars, how often would you say you get carsick?

Always_____ Frequently_____ Sometimes_____ Rarely_____ Never_____

12) Have you ever experienced any sort of simulator sickness?

Yes_____ No_____ If yes, describe the simulator and simulation:

Describe the symptoms. Include how long they lasted:

What do you think caused the problem:

13) Indicate a preference for the following devices/situations and circle any symptoms of motion sickness that your have experienced using them.

Aircraft

Like_____ Dislike _____ Neutral_____

Symptoms: none, headache, awareness of breathing, vertigo, pallor, sweating, drowsiness, dizziness, salivation, stomach awareness, nausea, vomiting, other:_____

Automobiles

Like_____ Dislike _____ Neutral_____

Symptoms: none, headache, awareness of breathing, vertigo, pallor, sweating, drowsiness, dizziness, salivation, stomach awareness, nausea, vomiting, other:_____

Cinerama or Wide-Screen Movies

Like_____ Dislike _____ Neutral_____

Symptoms: none, headache, awareness of breathing, vertigo, pallor, sweating, drowsiness, dizziness, salivation, stomach awareness, nausea, vomiting, other:_____

Elevators

Like_____ Dislike _____ Neutral_____

Symptoms: none, headache, awareness of breathing, vertigo, pallor, sweating, drowsiness, dizziness, salivation, stomach awareness, nausea, vomiting, other:_____

Long train or bus trips

Like_____ Dislike _____ Neutral_____

Symptoms: none, headache, awareness of breathing, vertigo, pallor, sweating, drowsiness, dizziness, salivation, stomach awareness, nausea, vomiting, other:_____

Merry-go-round

Like_____ Dislike _____ Neutral_____

Symptoms: none, headache, awareness of breathing, vertigo, pallor, sweating, drowsiness, dizziness, salivation, stomach awareness, nausea, vomiting, other:_____

Swings

Like_____ Dislike _____ Neutral_____

Symptoms: none, headache, awareness of breathing, vertigo, pallor, sweating, drowsiness, dizziness, salivation, stomach awareness, nausea, vomiting, other:_____

14) Have you ever been motion sick under any conditions other than the ones listed?

Yes_____ No_____ If yes, under what conditions:

15) If you were in an experiment where 50% of the subjects get sick, what do you think your chances of getting sick would be?

Certainly _____ Probably_____ Not sure_____ Probably not_____ Certainly not_____

PRE-SESSION ASSESSMENT

1) Have you been ill in the past week?

   Yes _____ No _____ If yes, please provide the following information:

   Nature and length of illness (include major symptoms):

   Are you fully recovered? Yes _____ No _____

2) How much alcohol have you consumed in the last 24 hours?

   # Beers _____ Ounces of Wine _____ Ounces of hard liquor _____

3) Please indicate any medication you have used in the past 24 hours:

   None _____

   Sedatives or tranquilizers _____

   Aspirin, Tylenol, other analgesics _____

   Anti-histamines _____

   Decongestants _____

   Other _____

   Specify:

4) How many hours sleep did you get last night?

   Hours _____

5) Please list any other comments regarding your present physical state which might affect your performance.

6) Assess your physical condition by circling the appropriate response below for each symptom.

General discomfort	None	slight	moderate	Severe
Fatigue	None	slight	moderate	Severe
Boredom	None	slight	moderate	severe
Drowsiness	None	slight	moderate	severe
Headache	none	slight	moderate	severe
Eye strain	none	slight	moderate	severe
Difficulty focusing	none	slight	moderate	severe
Increased salivation	none	slight	moderate	severe
Decreased salivation	none	slight	moderate	severe
Sweating	none	slight	moderate	severe
Nausea	none	slight	moderate	severe
Difficulty concentrating	none	slight	moderate	severe
Mental depression	none	slight	moderate	severe
"Fullness of the Head"	none	slight	moderate	severe
Blurred vision	none	slight	moderate	severe
Dizziness with eyes open	none	slight	moderate	severe
Dizziness with eyes closed	none	slight	moderate	severe
Vertigo[1]	none	slight	moderate	severe
Visual flashbacks[2]	none	slight	Moderate	severe
Faintness	none	slight	moderate	severe
Over awareness of breathing	none	Slight	moderate	severe

[1] Vertigo is experienced as loss of orientation with respect to vertical upright.
[2] Visual illusion of movement or false sensations.

Stomach awareness[1]	none	slight	Moderate	severe
Loss of appetite	none	slight	Moderate	severe
Increased appetite	none	slight	moderate	Severe
Bowels	none	Slight	moderate	severe
Confusion	none	slight	moderate	severe
Burping	none	slight	moderate	Severe
Other				

[1] Stomach awareness is usually used to indicate a feeling of discomfort which is just short of nausea.

POST-SESSION ASSESSMENT

1) Assess your physical condition by circling the appropriate response below for each symptom.

General discomfort	none	slight	moderate	severe
Fatigue	none	slight	moderate	severe
Boredom	none	slight	moderate	severe
Drowsiness	none	slight	moderate	severe
Headache	none	slight	moderate	severe
Eye strain	none	slight	moderate	severe
Difficulty focusing	none	slight	moderate	severe
Increased salivation	none	slight	moderate	severe
Decreased salivation	none	slight	moderate	severe
Sweating	none	slight	moderate	severe
Nausea	none	slight	moderate	severe
Difficulty concentrating	none	slight	moderate	severe
Mental depression	none	slight	moderate	severe
"Fullness of the Head"	none	slight	moderate	severe
Blurred vision	none	slight	moderate	severe
Dizziness with eyes open	none	slight	moderate	severe
Dizziness with eyes closed	none	slight	moderate	severe
Vertigo[1]	none	slight	moderate	severe
Visual flashbacks[2]	none	slight	moderate	severe
Faintness	none	slight	moderate	severe

[1] Vertigo is experienced as loss of orientation with respect to vertical upright.
[2] Visual illusion of movement or false sensations.

Over awareness of breathing	none	slight	moderate	severe
Stomach awareness[1]	none	slight	moderate	severe
Loss of appetite	none	slight	moderate	severe
Increased appetite	none	slight	moderate	severe
Desire to move bowels	none	slight	moderate	severe
Confusion	none	slight	moderate	severe
Burping	none	slight	moderate	severe

Other:

1) If symptoms were experienced, what do you think caused them?

2) Describe any unusual events that occurred during your session?

3) Describe any problems you observed in the visual presentation of information.

4) Describe any other problems you encountered.

---

[1] Stomach awareness is usually used to indicate a feeling of discomfort that is just short of nausea.

POST-EXPERIMENT QUESTIONNAIRE

Circle the response that describes your agreement or disagreement with the following statements.

1) I believed in the virtual reality illusion, felt a sense of presence in the environments, and felt immersed in the virtual worlds.

   1 - Strongly agree 2 - Agree 3 - Somewhat agree 4 - Indifferent 5 - Somewhat disagree 6 - Disagree 7 - Strongly disagree

2) I use computers often.

   1 - Strongly agree 2 - Agree 3 - Somewhat agree 4 - Indifferent 5 - Somewhat disagree 6 - Disagree 7 - Strongly disagree

3) I enjoyed the experiment.

   1 - Strongly agree 2 - Agree 3 - Somewhat agree 4 - Indifferent 5 - Somewhat disagree 6 - Disagree 7 - Strongly disagree